



THE UNIVERSITY *of* EDINBURGH

Edinburgh Research Explorer

An Invertron-Like Linear Plasmid Mediates Intracellular Survival and Virulence in Bovine Isolates of *Rhodococcus equi*.

Citation for published version:

Valero-Rello, A, Hapeshi, A, Anastasi, E, Alvarez, S, Scotti, M, Meijer, WG, MacArthur, I & Vazquez-Boland, JA 2015, 'An Invertron-Like Linear Plasmid Mediates Intracellular Survival and Virulence in Bovine Isolates of *Rhodococcus equi*.', *Infection and Immunity*, vol. 83, no. 7, pp. 2725-2737.
<https://doi.org/10.1128/IAI.00376-15>

Digital Object Identifier (DOI):

[10.1128/IAI.00376-15](https://doi.org/10.1128/IAI.00376-15)

Link:

[Link to publication record in Edinburgh Research Explorer](#)

Document Version:

Peer reviewed version

Published In:

Infection and Immunity

Publisher Rights Statement:

This is the author's final manuscript as accepted for publication

General rights

Copyright for the publications made accessible via the Edinburgh Research Explorer is retained by the author(s) and / or other copyright owners and it is a condition of accessing these publications that users recognise and abide by the legal requirements associated with these rights.

Take down policy

The University of Edinburgh has made every reasonable effort to ensure that Edinburgh Research Explorer content complies with UK legislation. If you believe that the public display of this file breaches copyright please contact openaccess@ed.ac.uk providing details, and we will remove access to the work immediately and investigate your claim.



An invertron-like linear plasmid mediates intracellular survival and virulence in bovine isolates of *Rhodococcus equi*

**Ana Valero-Rello^a, Alexia Hapeshi^a, Elisa Anastasi^b, Sonsiray Alvarez^b,
Mariela Scotti^{a,b}, Wim G. Meijer^c, Iain MacArthur^b, Jose A. Vazquez-Boland^{a,b,d,*}**

Microbial Pathogenesis Unit, School of Biomedical Sciences and Centre for Immunity,
Infection and Evolution, University of Edinburgh, UK^a; Division of Infection & Immunity, Roslin
Institute, University of Edinburgh, UK^b; School of Biomolecular and Biomedical Science,
University College Dublin, Dublin, Ireland^c; Grupo de Patogenómica Bacteriana, Facultad de
Veterinaria, Universidad de León, León, Spain^d

Running title: *R. equi* bovine-associated virulence plasmid pVAPN

* Corresponding author at: The Roslin Institute, Easter Bush, Edinburgh EH25 9RG,
Scotland, UK. Tel.: +44(0)131 651 3619; Fax: +44(0)131 651 9105. E-mail address:
v.boland@ed.ac.uk

50 **ABSTRACT**

51 We report a novel host-associated virulence plasmid in *Rhodococcus equi*, pVAPN, carried by
52 bovine isolates of this facultative intracellular pathogenic actinomycete. Surprisingly, pVAPN
53 is a 120-kb invertron-like linear replicon unrelated to the circular virulence plasmid associated
54 with equine (pVAPA) and porcine (pVAPB variant) *R. equi* isolates. pVAPN is similar to the
55 linear plasmid pNSL1 from *Rhodococcus* sp. NS1 and harbors six new *vap* multigene family
56 members (*vapN* to *-S*) in a *vap* pathogenicity locus acquired via en-bloc mobilization from a
57 direct predecessor of the equine pVAPA. Loss of pVAPN rendered *R. equi* avirulent in
58 macrophages and mice. Mating experiments using an *in vivo* transconjugant selection strategy
59 demonstrated that pVAPN transfer is sufficient to confer virulence to a plasmid-cured *R. equi*
60 recipient. Phylogenetic analyses distributed the *vap* multigene family complement from
61 pVAPN, pVAPA and pVAPB in seven monophyletic clades, each containing plasmid type-
62 specific allelic variants of a precursor *vap* gene carried by the nearest *vap* island ancestor.
63 Deletion of *vapN*, the predicted “bovine-type” allelic counterpart of *vapA* essential for
64 virulence in pVAPA, abrogated pVAPN-mediated intramacrophage proliferation and
65 virulence in mice. Our findings support a model in which *R. equi* virulence is conferred by
66 host-adapted plasmids. Their central role is mediating intracellular proliferation in
67 macrophages, promoted by a key *vap* determinant present in the common ancestor of the
68 plasmid-specific *vap* islands, with host tropism as a secondary trait selected during co-
69 evolution of individual virulence plasmids with specific animal species.

70

71 *Rhodococcus equi* is a gram-positive aerobic coccobacillus of the *Actinomycetales* associated
72 with chronic or subacute pyogenic infections (1, 2). A normal soil inhabitant, the bacterium
73 uses manure as a growth substrate, multiplies in the herbivore's large intestine and is
74 ubiquitous in the farm environment. Transmission occurs via contaminated dust particles,
75 mostly through airborne exposure (3, 4). *R. equi* is the causative agent of a major infectious
76 disease of the horse that affects young foals worldwide. The infection is characterized by
77 multifocal purulent bronchopneumonia, often accompanied by ulcerative or abscessating
78 lesions in the intestine (1, 5). While most well known as an equine pathogen, *R. equi* also
79 infects other animal species (1, 6-8). In abattoir surveys, *R. equi* is frequently recovered from
80 porcine submaxillary lymph nodes with granulomatous lesions as well as from apparently
81 healthy pigs (9-11). In cattle, it is typically isolated from caseating abscesses in respiratory
82 lymph nodes resembling bovine tuberculosis (TB) lesions (12). *R. equi* is also recognized as
83 an opportunistic pathogen in humans, where it causes severe TB-like purulent cavitary
84 pneumonia, bacteremia and extrapulmonary localized infections (8, 13, 14).

85 *R. equi* pathogenesis depends on the capacity of the bacterium to survive and replicate
86 within host macrophages (15-18). In equine isolates, this ability is conferred by a conjugative
87 circular plasmid of 80 kb (19-21) that promotes intravacuolar survival by interfering with
88 phagosome maturation (22). These properties are mediated by the *vap* pathogenicity island
89 (PAI) (23), a horizontal gene transfer (HGT) locus (24). A hallmark of the *vap* PAI is the
90 presence of a multigene family encoding homologous virulence-associated proteins (Vap)
91 (20, 24, 25). One of them, VapA, a 19 kDa secreted protein, is essential for virulence. A
92 single *vapA* gene deletion causes strong attenuation comparable to that caused by loss of the
93 plasmid, with both an inability to proliferate in macrophages and to survive *in vivo* in mice
94 (26, 27).

95 Emerging evidence suggests that the virulence plasmid may also play a key role in *R.*
96 *equi* host tropism. Early studies showed that VapA-encoding virulence plasmids were typical

97 of equine strains (28, 29), while a second plasmid type encoding VapB, a VapA variant (24),
98 was common among non-equine (pig and human) isolates (10, 30-33). Recently, the existence
99 of a third type of *R. equi* virulence plasmid was identified in bovine and human isolates
100 initially deemed to be “plasmidless” because negative for the *vapA* and *vapB* gene markers,
101 but which tested positive for a *traA* plasmid conjugal transfer gene marker (34). Molecular
102 epidemiological analysis of a global collection of *R. equi* isolates established that the *vapA*⁺,
103 *vapB*⁺ and novel *vapAB*⁻ plasmid types were each associated with a specific non-human host,
104 i.e. equine, porcine and bovine, respectively (34). Using a unified nomenclature these
105 plasmids were designated, respectively, pVAPA, pVAPB and pVAPN (for “noA-noB”
106 virulence plasmid) (1, 24). In contrast to their unique animal species specificity, the three
107 host-adapted plasmid types were commonly detected in human isolates. Besides pointing to a
108 zoonotic origin of the infection, this lack of plasmid type selectivity was consistent with
109 humans being an opportunistic, non-adapted host for *R. equi* (34).

110 Sequencing of the pVAPA and pVAPB virulence plasmids revealed they are
111 essentially the same circular replicon (24). The analyzed plasmids, pVAPA1037 and
112 pVAPB1593 (numerical suffix indicating the source strain according to recently suggested
113 harmonized nomenclature for *R. equi* virulence plasmids) (24), shared a virtually identical
114 backbone encoding replication/partitioning and conjugal transfer functions. In contrast, the
115 *vap* PAI was more divergent, differing both in size and *vap* gene complement, i.e. ≈21 kb and
116 nine *vap* genes for pVAPA (*vapA*, -*C*, -*D*, -*E*, -*G* and -*H* and the pseudogenes *vapF*, -*I* and -*X*)
117 vs ≈15 kb and six *vap* genes for pVAPB (*vapB*, -*J*, -*K1*, -*K2*, -*L* and -*M*) (24). In addition to
118 major Vap polypeptide sequence diversification, *vap* multigene family re-arrangements
119 (duplications and translocations) and insertion/deletions affecting adjacent genes accounted
120 for the PAI differences. This suggested that the *vap* PAIs were evolving at a faster rate than
121 the conserved housekeeping backbone, consistent with diversifying selection and a possible
122 role in host-specific adaptation (24).

123 Here, we report the genomic analysis and characterization of pVAPN, the bovine-type
124 *R. equi* virulence plasmid.

125

126 **MATERIALS AND METHODS**

127 **Strains, culture conditions and reagents.** *R. equi* PAM1571 is a prototypic *traA*⁺/*vapAB*⁻
128 bovine strain (34) isolated from a heifer's mediastinal lymph node with pyogranulomatous
129 lesions (kindly provided by F. Quigley, Central Veterinary Research Laboratory, Ireland)
130 (12). Its plasmid-cured derivative PAM1571⁻ was obtained by subjecting the wild-type
131 bacteria to an electroporation pulse of 12.5 kV/cm, 1000 Ω and 25 μF (GenePulser Xcell,
132 BioRad) followed by six cycles of plating and single-colony subculturing in liquid medium at
133 37 °C (27). These two strains are henceforth designated 1571 and 1571⁻, respectively. *R. equi*
134 PAM2012 is another *traA*⁺/*vapAB*⁻ bovine strain, isolated in Germany from a case of
135 lymphadenitis in cattle (kindly provided by C. Lämmler, Veterinary Faculty, University of
136 Giessen) (35). *R. equi* 103S is the reference genome strain, a low passage clone of equine
137 clinical isolate 103⁺ used in different laboratories worldwide (24). Its isogenic 103SΔ*vapA*
138 and plasmid-cured 103S⁻ derivatives have been described elsewhere (27). The presence of the
139 virulence plasmid was routinely checked in all strains by PCR using suitable oligonucleotide
140 primer combinations (Table S1). *R. equi* was grown in brain-heart infusion (BHI, Difco-BD)
141 or Luria-Bertani (LB, Sigma) media at 30 °C unless stated otherwise. The cloning host strain
142 *Escherichia coli* DH5α was grown at 37 °C in LB. Media were supplemented with 1.5% agar
143 (w/v) and/or antibiotics as appropriate. Fluid cultures were incubated with shaking (200 rpm).
144 Chemicals and primers were purchased from Sigma-Aldrich unless stated otherwise.

145 **DNA techniques.** Total DNA extraction and purification from *R. equi*, PCR
146 techniques, DNA fragment purification and electrophoresis, recombinant DNA techniques,
147 and plasmid purification and electroporation, were performed as previously described (27, 34,
148 36). For pulsed-field DNA electrophoresis (PFGE), plugs were formed by embedding *R. equi*

149 cells from 1-ml 24-h BHI culture aliquots in melted 1% agarose in TE buffer. Plugs were
150 incubated in lysozyme solution (10 mM Tris-HCl pH 8.0, 50 mM NaCl, 1 mg/ml lysozyme)
151 at 37°C for 2 h, washed in 20 mM Tris-HCl pH 8.0, 50 mM EDTA and incubated in
152 proteinase K solution (10 mM TrisHCl pH 8.0, 100 mM EDTA, 0.2 g/ml sucrose, 1 mg/ml
153 proteinase K) at 50 °C overnight. Plugs were then loaded into 1% Pulsed Field Certified™
154 agarose gel (BioRad) prepared with 0.5× Tris-borate-EDTA buffer (TBE). DNA was
155 separated in a CHEF-DR(R) II Pulsed Field Electrophoresis System (BioRad) at 5 V/cm²
156 voltage, switch time ramping from 20 to 30 s, and 23 h run time at 14°C. Southern blotting
157 was performed by transferring resolved DNA fragments to a positively-charged nylon
158 membrane after treatment of the PFGE gels with 0.25 M HCl for 30 min followed by
159 denaturing solution (1.5 M NaCl, 0.4 M NaOH) for 20 min (twice) and neutralizing solution
160 (1.5 M NaCl, 0.5 M TrisCl₂ pH 7.0) for 20 min (twice). Membranes were hybridized using a
161 specific *vapN-vapQ* PCR fragment (Table S1) labelled with digoxigenin (DIG High Prime
162 DNA Labeling and Detection Kit, Roche).

163 **pVAPN sequencing and phylogenetic analyses.** pVAPN1571 was electroeluted from
164 preparative PFGE gels using a Model 422 apparatus and (BioRad) and pair-end (2× 36-bp)
165 sequenced in an Illumina (Solexa) II Genome Analyzer at Edinburgh Genomics facility. To
166 complete the plasmid assembly, the host strain 1571 was paired-end (2× 100-bp) sequenced
167 from a 500 bp PCR-free library using an Illumina HiSeq 2000 Sequencing System at Beijing
168 Genomics Institute. pVAPN2012 was entirely sequenced using the latter approach. Reads
169 were assessed for quality using FASTQC, then trimmed for adaptors using SCYTHE and for low
170 quality reads using SICKLE. *De novo* assembly was performed using SPADES followed by
171 manual verification by PCR mapping and Sanger re-sequencing of specific regions. The 5'
172 end telomeric sequence of pVAPN was experimentally confirmed as previously described
173 (37) using the suicide vector pSelAct (38) and the vector-encoded apramycin resistance for
174 selecting positive clones. The pVAPN sequence was manually curated and annotated in

175 ARTEMIS using the software and databases listed in Table S2. For phylogenetic analyses,
176 orthologs were identified by reciprocal tBLASTX analysis with 30% identity over >60% of the
177 protein sequence as minimum similarity score. Paralogous genes predicted based on the
178 topology of Neighbor joining trees and pseudogenes (except *vap* pseudogenes) were avoided.
179 Translated products from each ortholog cluster were MUSCLE-aligned (except otherwise
180 stated) and back-translated in MEGA5, and best evolutionary model for nucleotide substitution
181 was selected according to AIC criterion in JMODELTEST. For Multilocus Sequence Alignment
182 (MLSA), gene alignments were concatenated with SEAVIEW. Maximum Likelihood (ML)
183 trees were constructed in PHYML. See Table S2 for bioinformatics and phylogenetic analysis
184 software references/urls.

185 **Construction of *vapN* deletion mutant.** The *vapN* gene was in-frame deleted from
186 pVAPN by double homologous recombination (36) using 5-fluorocytosine counter-selection
187 (38). Briefly, oligonucleotide primer pairs Nmutant_a (EcoRI)/Nmutant_b1 (XmaI) and
188 Nmutant_c1 (XmaI)/Nmutant_d (SpeI) (Table S1) were used to PCR-amplify two DNA
189 fragments of 908 and 910 bp carrying the last three 5'-terminal and four 3'-terminal codons of
190 *vapN* plus adjacent upstream and downstream regions, respectively. The PCR products were
191 joined via the XmaI site introduced by the Nmutant_b1 and Nmutant_c1 primers, the ligation
192 product inserted into the pSelAct vector (38) using the external SpeI and EcoRI sites
193 introduced by the primers Nmutant_a and Nmutant_d, and the resulting plasmid
194 electroporated into 1571. Allele exchange was monitored by PCR mapping using suitable
195 primers (Table S1) and the in-frame deletion confirmed by DNA sequencing on both strands.

196 **Mating experiments.** Transfer of the virulence plasmid between *R. equi* bacteria was
197 investigated using a mating protocol essentially as previously described (39). Overnight BHI
198 cultures of donor and recipient *R. equi* were harvested by centrifugation, resuspended in
199 phosphate-buffered saline (PBS) to a cell density of $\approx 10^7$ CFU, mixed $\approx 1:1$ and spotted in a
200 ≈ 5 μ l drop onto BHI agar. The recipient 103S⁻ bacteria carried a chromosomal rifampicin

201 resistance (Rmp^R) marker. 103S^{-Rmp^R} bacteria were isolated by selection of spontaneous
202 resistant mutants on increasing concentrations of rifampicin, from 25 to 100 µg/ml, and
203 stabilization by repeated subculturing in the presence of the highest concentration of the
204 antibiotic. After incubating the mating mixture at 30 °C for 72 h, bacteria were collected in 1
205 ml of PBS, serially diluted, and plated onto BHI agar without and with supplementation with
206 100 µg/ml rifampicin. At this rifampicin concentration, no Rmp^R colonies were detected in
207 the only-donor control plates. Transconjugants were identified among Rmp^R colonies by
208 simultaneous PCR detection of virulence plasmid-specific markers and of recipient's
209 chromosomal gene markers (103S strain-specific sequences identified from genome
210 comparisons) using *ad hoc* oligonucleotide primers (Table S1).

211 **Macrophage cultures and infection assay.** Low-passage murine J774A.1
212 macrophages and human monocyte-like THP-1 cells were obtained from ATCC and cultured
213 at 37 °C under 5 % CO₂ in Dulbecco's minimal essential medium supplemented with 10% de-
214 complemented fetal bovine serum, 2 mM glutamine and 1 mM pyruvate (DMEM). THP-1
215 cells were initially grown in suspension in RPMI-1640 medium with the same supplements.
216 Cells were seeded on 24-well plates at a density of $\approx 2 \times 10^5$ cells/well and incubated overnight
217 in DMEM, for THP-1 monocytes in the presence of 50 ng/ml phorbol 12-myristate 13-acetate
218 (PMA) to allow differentiation into macrophages. Infection assays were performed on $\approx 80\%$
219 confluent macrophage monolayers as previously described (40). Intracellular proliferation
220 data were normalized to the initial counts at $t = 0$ using an "Intracellular Growth Coefficient"
221 according to the formula: $IGC = (IB_n - IB_0) / IB_0$, where IB_n and IB_0 are the intracellular
222 bacterial numbers at $t = n$ and $t = 0$, respectively (40, 41).

223 **Mouse infections.** Experiments were performed at the Animal Facility of the School
224 of Biological Sciences of the University of Edinburgh using in-house-bred six- to eight-week-
225 old BALB/c mice. Mouse intranasal and intravenous infections and the lung competitive
226 virulence assay were performed as previously described (27). The relative proportion of the

competing bacteria was calculated by analyzing at least 40 random colonies from the plated organ homogenate by PCR using suitable oligonucleotide primers (Table S1). Competitive index values were calculated using the formula $C.I. = (\text{test/reference log CFU ratio at } t = n) / (\text{input test/reference log CFU ratio in inoculum})$ (27). Mouse experiments were approved by the University of Edinburgh's Ethical Review Committee and were covered by a Project License granted by the UK Home Office under the Animals (Scientific Procedures) Act 1986.

Statistics. Intracellular proliferation and uptake data were compared using two-way and one-way ANOVA, respectively, followed by Šidák post-hoc multiple comparison tests. One-sample Student's *t* tests were used to determine if C.I. values differed significantly from 1 (i.e. the expected C.I. value if the ratio of the competing strains remains the same respect to $t = 0$). Statistical analyses were performed using Prism 6.0 software (GraphPad, San Diego, CA).

RESULTS AND DISCUSSION

Identification and sequencing of pVAPN. Attempts to isolate the novel *traA*⁺/*vapAB*⁻ plasmid type (34) from 1571 and other bovine isolates using the procedure for *R. equi* circular virulence plasmid extraction (34) were unsuccessful. However, PFGE analysis of undigested genomic DNA revealed a distinct band in the range of ≈100 Kb in all bovine strains from our collection ($n = 22$). This band was not detected in *R. equi* strains carrying a circular virulence plasmid e.g. 103S harboring pVAPA (Fig. 1). Similarity searches of exploratory low-coverage whole-genome 454 pyrosequencing assemblies from 1571 with the pVAPA reference sequence from *R. equi* 103S (40) identified contigs harboring *vap* PAI-homologous genes. Southern blotting using a probe from this novel *vap* PAI identified the ≈100 Kb PFGE band as the putative pVAPN virulence plasmid (Fig. 1). Most (95%) tested *traA*⁺/*vapAB*⁻ bovine isolates (34) were positive for pVAPN by PCR using a plasmid-specific *vap* PAI marker (*vapN*, the counterpart of the equine *vapA* and porcine *vapB*, see below). The ≈100-

253 Kb band from strain 1571 was isolated from PFGE gels and shotgun sequenced. The
254 pVAPN1571 genome sequence was completed as described in Materials & Methods.
255 pVAPN1571 is 119,931 bp long and contains 148 open reading frames (ORFs), of
256 which 10 are pseudogenes (Fig. 2). The average G+C content is 66.2 %, similar to that of *R.*
257 *equi* genomic DNA (68.7%) (40). pVAPN1571 is predicted to be a linear replicon based on
258 its PFGE migration pattern (42), presence of a *traB* conjugal translocase determinant (see
259 below), phylogenetic relatedness with other *Rhodococcus* linear plasmids (Fig. 3A), and
260 presence of telomeric invertron-like terminal inverted repeats (TIR) with multiple palindromic
261 secondary structures (Fig. 4) (43-45). pVAPN's TIR sequences are 569 bp-long and 99%
262 identical. The nucleotide sequence of a second example of pVAPN plasmid, from a bovine
263 isolate from Germany (PAM2012), was virtually identical to that of pVAPN except for the
264 presence of two additional ORFs before the left telomeric sequence (Fig. S1). The
265 pVAPN1571 and pVAPN2012 genome sequences have been deposited in GenBank under
266 Accession Nos. KF439868 and KP851975, respectively

267 **Comparative analysis and functional overview.** *Rhodococcus* species
268 characteristically possess large plasmids, circular or linear if >100 Kb in size (46). They
269 consist of a vertically evolving backbone, encoding plasmid maintenance and conjugal
270 transfer functions, and a horizontally acquired variable region (VR) providing specific niche-
271 adaptive properties to the host bacterium (24, 37, 44, 45, 47). The housekeeping backbone of
272 pVAPN is unrelated to that of the circular pVAPA/B (equine/porcine type) *R. equi* virulence
273 plasmids. pVAPN instead is closely related to the linear plasmid pNSL1 from *Rhodococcus*
274 sp. NS1 (48) in terms of genetic structure and synteny (Fig. 2). pNSL1 is of a similar size
275 (117, 252 bp) and perfectly colinear with pVAPN. No significant overall similarity was
276 detected with other sequenced linear plasmids from the genus *Rhodococcus* in pairwise
277 alignments (Fig. S3). However, a phylogenetic multilocus sequence analysis (MLSA) of gene
278 orthologs from the housekeeping backbones of a representation of rhodococcal linear and

279 circular plasmids placed pVAPN within a monophyletic clade together with the linear
 280 replicons, indicating they all share a common origin (Fig. 3A).

281 *Conjugation genes.* pVAPN encodes a MOBf (TrwC)-family conjugal relaxase (49)
 282 homologous to TraA from pVAPA/B (24). Detection of its coding sequence (pVAPN_0650)
 283 by PCR using conserved *traA* target sequences from pVAPA/B allowed the discovery of the
 284 *traA*⁺/*vapAB*⁻ bovine pVAPN plasmid in a first instance (34). Relaxases play a key role in the
 285 conjugation of circular plasmids, nicking the supercoiled dsDNA and leading the nascent
 286 DNA strand into the recipient cell in conjunction with a type IV secretion system (T4SS),
 287 which forms the transport channel (50, 51). Indeed, deletion of *traA* has been shown to
 288 prevent the transfer of the equine pVAPA circular virulence plasmid (39). Interestingly,
 289 however, the pVAPN *traA* relaxase gene is corrupted (5' terminal deletion affecting the first
 290 75 codons including gene start and part of TrwC relaxase domain, frameshifts in the 3'
 291 terminal region) and probably non-functional. This *traA* pseudogene is located outside the
 292 pVAPN conjugation module at the left boundary of the *vap* PAI. It is immediately contiguous
 293 to three ORFs encoding phage excisionase, Rep and CopG (regulator of plasmid copy
 294 number) homologs, also present in the pVAPA/B backbone (24). These three ORFs and
 295 adjacent pVAPN *vap* PAI are identified as HGT by the ALIEN_HUNTER program, which
 296 detects putative horizontally acquired genetic material based on local compositional bias (52)
 297 (Fig. 2). This suggests that the *traA* pseudogene-phage excisionase-*rep-copG* genes (absent
 298 from pNSL1) are remnants of a lateral gene exchange –probably the same that mobilized the
 299 *vap* PAI locus– between the circular virulence plasmid and pVAPN.

300 Despite *traA* being a pseudogene and a relaxase-associated T4SS apparatus being
 301 absent, pVAPN is transferable by mating (see below). This is probably mediated by
 302 pVAPN_0320 encoding a TraB plasmid translocase, also present in pNSL1. TraB
 303 translocases are evolutionarily related to the septal FtsK/SpoIIE-family proteins involved in
 304 chromosome segregation (51) and have been recently shown to mediate a novel relaxase-

305 /T4SS-independent mechanism of conjugation in *Streptomyces* linear replicons (53). They all
306 share a similar structural arrangement, with an AAA+ motor ATPase domain with
307 characteristic Walker A and B boxes, a transmembrane domain and a C-terminal DNA-
308 binding winged helix-turn-helix motif (53). In translocase-mediated conjugation, TraB binds
309 to the plasmid's dsDNA and forms a transmembrane DNA-conducting hexameric channel
310 through which the plasmid is transferred to the recipient bacterium in an ATP-dependent
311 manner. The pVAPN (and pNSL1) conjugation module also comprises (i) an additional
312 AAA+ ATPase with sequence similarity to the conjugative coupling factor TraD
313 (pVAPN_0360); (ii) a homolog of a Soj/ParA-family ATPase (pVAPN_0300), involved in
314 chromosomal and plasmid DNA segregation (54) and recruitment of conjugative DNA to the
315 transfer channel (55); (iii) a putative M23 endopeptidase family/lysozyme-like lytic murein
316 transglycosylase/cell wall hydrolase (pVAPN_0390), probably involved in conjugation
317 channel formation (of which a homolog is also present in the circular pVAPA/B virulence
318 plasmids and related *R. erythropolis* pREC1) (Fig. 2); and (iv) a number of putative
319 membrane-associated proteins. In addition, pVAPN_0550, at the other side of an interposed
320 plasmid replication/partitioning (*rep-parA*) module, encodes a putative cutinase. A cutinase
321 gene is also present at the boundary of this replication/partitioning module and the
322 conjugation module in the circular pVAPA/B and pREC1 replicons (Fig. 2). Bacterial
323 cutinase-like proteins, common among mycolic-acid containing actinomycetes (40, 56), have
324 esterase/lypolytic activity (56-58). In mycolata-infecting phages they form part of the LysB
325 lipolytic enzyme complement, thought to aid in the breakdown of the lipid-rich envelope
326 during phage penetration or lytic egress (59). Recently, a cutinase from *R. fascians* pFiD188
327 linear virulence plasmid has been shown to be required for efficient conjugation, probably by
328 facilitating the penetration of the DNA translocation complex in the rhodococcal cell
329 envelope (45).

330 *Replication/partitioning.* The pVAPN self-replication determinant includes a module
 331 encoding a Rep protein (pVAPN_0480), which probably directs the bidirectional replication
 332 of the plasmid towards the telomeres, and the plasmid partitioning protein/ATPase ParA
 333 (pVAPN_0500). A 26-bp semi-palindromic sequence (5'-
 334 AAAACCCCCAGGTGGGGGTGGG- TTTT) similar to that determined as the origin of
 335 replication of the pNSL1 plasmid (48) was identified at the same position upstream from the
 336 *rep* gene in pVAPN (Fig. 2). The *rep-parA* module is detected as HGT genetic material in
 337 pNSL1 and is conserved in the circular plasmids pVAPA/B and *R. erythropolis* pREC1 (in
 338 the latter also identified as HGT). In pVAPN, it is flanked on the right by a phage excisionase
 339 gene (pVAPN_0520) which is conserved in pNSL1 and, interestingly, also in the circular
 340 replicons despite these deriving from a different ancestor (Fig. 2). This lends additional
 341 support to the earlier suggestion that the *rep-parA* determinant forms part of an
 342 “exchangeable” gene cassette subjected to HGT between different rhodococcal plasmids (24).
 343 This replication/partitioning region appears to serve as an insertion platform for HGT DNA
 344 (24), as suggested by the fact that the VR is either immediately adjacent (pVAPA/B circular
 345 plasmids) or interrupts it (pVAPN, pNSL1 and the larger circular pREC1) (Fig. 2).
 346 Interestingly, in contrast to the circular pVAPA/B plasmids (and pREC1), pVAPN (and
 347 related pNSL1) does not encode the ParB component of the ParAB replicon segregation
 348 system (60). The lack of a *parB* gene appears to be a hallmark of the smaller (≤ 400 Kb)
 349 rhodococcal linear extrachromosomal replicons, as exemplified by pREL1 or pBD2 from *R.*
 350 *erythropolis* (44), pRHL2 and pRHL3 from *R. jostii* (37) or pFiD188 from *R. fascians* (45).
 351 *Plasticity region (VR).* The colinearity with pNSL1 is abruptly interrupted at the level
 352 of the *traA* pseudogene, marking the start of the VR. pVAPN’s VR is interrupted by an island
 353 of homology with ORFs from the right end of pNSL1’s backbone, suggesting it has been
 354 formed by two independent DNA acquisition events (Fig. 2). The left VR section comprises
 355 the pVAPA/B-homologous phage excisionase-*rep-copG* sequence module (see above) plus

356 the *vap* PAI; the right section encodes rhodococcal/actinobacterial conserved hypothetical
357 proteins and a number of products with various predicted functions (Fig. 2). The complete left
358 VR section with the *vap* PAI is identified as HGT (Fig. 2), suggesting it is a more recent
359 acquisition.

360 ***vap* PAI.** pVAPN's *vap* PAI genetic structure is similar to that of pVAPA/B (Fig. 5).
361 It is 15.1 Kb in length and contains 21 ORFs including: (i) a complement of six *vap* genes
362 (*vapN*, -*O*, -*P*, -*Q* pseudogene, -*R* and -*S*) encoding polypeptides differing by 20 to 81% in
363 amino acid sequence identity with pVAPA/B's Vaps (Table S3); (ii) a *vir* locus encoding the
364 two key *vap* PAI transcriptional regulators, VirR (LysR-type) and VirS (orphan two-
365 component response regulator) (61, 62), a major facilitator superfamily (MFS) transporter
366 IcgA (63), plus VapP and a conserved protein of unknown function; and (iii) several
367 additional non-*vap* genes (Fig. 5). Four of the latter are conserved as functional genes in the
368 three virulence plasmids, indicating they are core components of the PAI: pVAPN_0700
369 (pVAPA/B_0420), encoding a hypothetical protein with similarity to a CopG-family
370 transcriptional regulator (here designated *cgf*), is the probable first gene of the *vap* PAI
371 instead of the downstream *lsr2* initially considered (24); pVAPN_0720 (pVAPA/B_0440),
372 encoding a putative nucleoid-associated protein similar to Lsr2, which in mycobacteria is
373 involved in a number of virulence-related functions (64-66); pVAPN_0760
374 (pVAPA/B_0470), encoding an S-adenosylmethionine (SAM)-dependent methyltransferase
375 with a potential regulatory role via protein, nucleic acid or lipid methylation; and
376 pVAPN_870 (pVAPA/B_0570), aka *vap*-coregulated *vcgB* gene in pVAPA, encoding a
377 hypothetical protein conserved in pathogenic mycobacteria (67) (Fig. 5). At the right end, the
378 putative transposon invertase/resolvase *invA* gene found in pVAPA/B and in the VR of the
379 related rhodococcal circular pREC1 plasmid (24), is replaced in pVAPN by *tmiA*-like
380 transposase/integrase and *tmiQ*-like transposase helper protein pseudogenes (Fig 5).

381 ***vap* PAI evolution.** A phylogenetic analysis of the *vap* multigene family was
382 performed to trace the evolutionary history of the *R. equi vap* PAI. Maximum Likelihood
383 (ML) trees grouped the *vap* genes into several well-supported terminal clades (Figs. 3B,
384 S4A). *vap* family members were not clustered by plasmid; instead, *vap* sequences from
385 different virulence plasmids were grouped under each of the nodes, suggesting they are allelic
386 variants of a vertically evolving *vap* precursor gene. Three of the clades contained *vap*
387 sequences from only one or two of the plasmid types, suggesting loss of *vap* alleles. In
388 addition, in two cases the clades included more than one *vap* sequence from the same PAI,
389 consistent with instances of *vap* gene duplication (Figs. 3B, S4A). To help pinpointing the
390 gene duplication and loss events underlying the evolution of the *R. equi vap* family, the *vap*
391 gene tree and a “species” tree of the three PAIs based on their conserved non-*vap* genes (Fig.
392 S4B) were compared using NOTUNG phylogenetic reconciliation software (68) (Fig. S5). The
393 phylogenetic data were then interpreted in combination with a detailed comparative analysis
394 of the genetic structure of the PAIs (Fig. 5).

395 The above analyses inferred that the lowest common ancestor (LCA) of the three *vap*
396 PAIs probably comprised seven precursor *vap* genes, designated 1 to 7. These gave rise to the
397 contemporary plasmid type-specific allelic variants as schematized in Fig. 3B (see also Figs.
398 S4A, S5 for additional details). The seven LCA *vap* gene precursors probably originated by
399 successive duplication events from a primordial *vap* gene (Figs. 6, S5), probably acquired by
400 HGT from another organism. Indeed, while being *R. equi*-specific among the actinomycetes,
401 Vap homologs are found in other bacteria from different phyla or even fungi (Fig. S4A).

402 The presence in pVAPN, adjacent to the PAI, of an orphan, corrupted copy of *traA* plus
403 other sequences from the pVAPA/B housekeeping backbone (phage excisionase-*rep-copG*
404 HGT sequence module) (Figs. 2, 5) suggests that the *vapN* PAI was mobilized to the linear
405 replicon from an ancestor of the circular pVAPA/B and not *vice versa*. An identical gene
406 translocation as that observed for the allelic variants *vapG* (pVAPA) and *vapO* (pVAPN) is

407 unlikely to have occurred twice independently, indicating that the *vapN* PAI probably
408 originated from a direct precursor of pVAPA after diversification from pVAPB. This
409 interpretation is supported by a phylogenetic analysis performed with the non-*vap* genes of
410 the PAI (Fig. S4B). It also accounts for the presence in the *vapN* PAI of pVAPA's *vapI/E* and
411 *vapC/F* putative allelic variants *vapR* and *vapS*, which are absent in pVAPB (Figs. 5, S5). The
412 *vapA* PAI deriving from pVAPN is less plausible because it implies the occurrence, after the
413 mobilization of the PAI, of a second, independent horizontal transfer/recombination event
414 conveying the *traA*-phage excisionase-*rep-copG* module from pVAPA/B to pVAPN. The
415 probable evolutionary history of the *vap* PAI in the three host-adapted *R. equi* virulence
416 plasmids is schematized in Fig. 6.

417 **pVAPN and its *vapN* gene are essential for intracellular proliferation in**
418 **macrophages.** To determine the role of pVAPN in virulence, we obtained an isogenic
419 plasmid-cured derivative of 1571 (1571⁻) and examined its behavior in *in vitro* infection
420 assays in mouse J774A.1 and human THP-1 macrophages. Studies with the equine plasmid
421 previously showed that VapA is essential for *R. equi* virulence (26, 27), in contrast to other
422 pVAPA-encoded Vap products (i.e. VapC, -D, -E, -F (26), -G (23) or -H [A. Hapeshi et al.,
423 unpublished]), which are dispensable or accessory. Since our data above suggest that *vapN* is
424 pVAPN's ortholog/allelic variant of *vapA*, an isogenic unmarked in-frame *vapN* deletion
425 mutant was also constructed and tested. A plasmidless derivative and a *vapA* deletion mutant
426 of equine isolate 103S (strains 103S⁻ and 103SΔ*vapA*, respectively) (27) were used as
427 controls.

428 Fig. 7A shows that both 1571⁻ and 1571Δ*vapN* had lost the ability to proliferate in
429 J774A.1 and THP-1 cells. The effects were essentially identical to those observed for 103S⁻
430 and 103SΔ*vapA*, respectively (Fig. 7B). These results demonstrate that the bovine plasmid
431 pVAPN is, like the equine pVAPA, necessary for facilitating *R. equi* parasitization of host
432 macrophages. They also show that *vapN* appears to perform an essential function in

433 pathogenesis, similar to *vapA* in the equine plasmid (26). Uptake of 1571⁻ and 1571Δ*vapN*
434 remained unaffected and the same was observed for 103S⁻ and 103SΔ*vapA* (Fig. S6),
435 indicating that the effect of the two plasmids and their cognate VapN and VapA products is
436 specifically related to intracellular survival and/or replication.

437 **Role of pVAPN and *vapN* in virulence *in vivo*.** The 1571 strain and its plasmidless
438 derivative 1571⁻ were also tested in mice using a competitive lung infection model (27).
439 Immunocompetent BALB/c mice were infected via the intranasal route with a ≈1:1 mix of the
440 test bacteria and *R. equi* burdens determined by plate counting over a four-day period, in
441 which we previously determined *R. equi* numbers remain stable in the lung (27). The relative
442 proportions of the two strains were then determined for each time point by PCR and the
443 corresponding competitive indexes (C.I.) calculated (see Materials & Methods).

444 Plasmidless 1571⁻ bacteria were cleared from the lungs at a much faster rate than the
445 1571 parent strain (Fig. 8A). Except for $t = 0$, when similar numbers of 1571 and 1571⁻ were
446 recovered, the C.I. was significantly lower than 1 at all time points (Table 1). By day 3 most
447 (96.3 %) of the bacteria were plasmid-positive whilst, at day 4, the 1571⁻ strain was not
448 detected despite total CFU numbers remaining stable in the lungs, indicating that the plasmid-
449 cured bacteria were strongly outcompeted (Fig. 8A). This pattern mirrored the results
450 observed when the same experiment was performed with *R. equi* 103S and its plasmidless
451 derivative 103S⁻ (27). These data demonstrate that the bovine-type pVAPN plasmid, like the
452 equine pVAPA, confers to *R. equi* the ability to survive *in vivo* in an animal host.

453 We next analysed the role of VapN in pVAPN-promoted virulence in mice. Since,
454 according to the macrophage data, the lack of VapN was likely to cause strong attenuation *in*
455 *vivo*, we compared the competitive ability of 1571Δ*vapN* against the non-virulent derivative
456 1571⁻ (27). This approach takes advantage of the greater sensitivity of competitive tests in
457 assessing small differences in virulence (69, 70) and, to ascertain the relative importance of

458 VapN and other pVAPN products in *R. equi* virulence, is potentially more informative than a
459 comparison with the fully virulent parent strain.

460 While the 1571⁻ strain was readily displaced by the plasmid-positive 1571, sizable
461 numbers of both $\Delta vapN$ and 1571⁻ were recovered at all time points (Fig. 8B). This is similar
462 to the behaviour of 103S $\Delta vapA$ and 103S⁻ using the same experimental conditions (27),
463 demonstrating that loss of VapN is sufficient to cause a reduction in virulence comparable to
464 that in the absence of its coding pVAPN plasmid. Nevertheless, the C.I. data showed partial
465 outcompetition of plasmid-cured 1571⁻ by $\Delta vapN$, particularly during the two first time points
466 (Table 1). No such differences were observed in our previous 103S $\Delta vapA$ vs 103S⁻
467 comparison (27). This indicates that pVAPN products other than VapN are also potentially
468 important for *R. equi* survival in mice, and that some differences might exist in the
469 contribution to virulence of VapN and VapA in their respective backgrounds.

470 Collectively, our data support the notion that VapN and VapA are allelic variants of a
471 same *vap* gene with a key role in *R. equi* virulence, presumably because essential for
472 supporting rhodococcal intramacrophage proliferation.

473 **pVAPN transferability by mating.** We finally tested whether pVAPN is transferable
474 by mating, as predicted from the sequence data. Experiments were carried out with the 1571
475 strain as donor and a rifampicin-resistant (Rmp^R) plasmidless 103S⁻ (103S^{-RmpR}) as recipient.
476 The two strains belong to different *R. equi* chromosomal genogroups (E. Anastasi et al.,
477 manuscript in preparation). As a control, conjugation tests with pVAPA from 103S, for which
478 transfer frequencies in the range of 10⁻² have been previously reported (39), were performed
479 using the same recipient. Transconjugants were determined by screening a total of 900
480 random Rmp^R (100 µg/ml) colonies using suitable recipient- and virulence plasmid-specific
481 PCR markers. Transfer of pVAPA to 103S⁻ was observed at a frequency of 1.25×10⁻² but
482 could not be detected for pVAPN. We reasoned that the linear pVAPN could be transferable
483 at a lower frequency, unworkable for the PCR-based screening method used. To circumvent

484 this, a transconjugant selection strategy was devised based on the ability of the virulence
485 plasmid to promote *R. equi* survival *in vivo*. BALB/c mice were infected intravenously (i.v.)
486 with $\approx 4 \times 10^8$ CFU of a mating mix of 1571 and 103S^{-Rmp^R}, followed by plating of spleen and
487 liver homogenates onto rifampicin plates at days 0, 3, and 5 after infection. Based on previous
488 i.v. infection data in mice (27), this time course was expected to lead to progressive
489 elimination of plasmid-negative *R. equi* and concomitant increase of the plasmid-positive
490 population. The recovered pVAPN-positive/Rmp^R bacteria were confirmed as transconjugants
491 by PCR using suitable strain-specific gene markers and determination of strain-specific DNA
492 sequences (see Table S1 and Materials & Methods).

493 Fig. 9A demonstrates a steady enrichment of pVAPN-positive transconjugants, from
494 0.5% at day 0 to 34.5% at day 3 and 80.3% at day 5. These data show that pVAPN is
495 transferable between different *R. equi* strains. The positive selection in mice of 103S⁻ pVAPN
496 transconjugants indicates that the bovine plasmid promotes *R. equi* virulence irrespective of
497 the strain hosting it. Experiments in J774A.1 cells demonstrated that acquisition of pVAPN is
498 sufficient to confer to *R. equi* the capacity for intracellular survival in macrophages (Fig. 9B).

499 **Conclusions.** Our previous work established that the equine-type pVAPA and
500 porcine-type pVAPB plasmids are the same circular replicon in which the HGT-acquired *vap*
501 PAI evolved divergently, presumably by host-driven selection (24). Our new data show that
502 the bovine pVAPN plasmid was originated by horizontal mobilization of the *vap* PAI to a
503 linear invertron-like replicon. The pVAPN *vap* locus, like pVAPA/B's, is an HGT island and
504 is flanked by DNA mobility genes, consistent with a recent lateral acquisition, probably
505 involving a phage or a transposon.

506 Both the circular pVAPA/B (24) and linear pVAPN backbones share a common origin
507 with other extrachromosomal conjugative replicons found in environmental rhodococci.
508 Rhodococcal plasmids play a key role in facilitating adaptation to different habitats and
509 environments via plasticity regions rich in HGT material. In the environmental biodegradative

510 rhodococci, these plasticity regions typically encode catabolic, detoxification or secondary
511 metabolic determinants while in the pathogenic species (*R. equi* and *R. fascians*) they are
512 virulence related (1, 46, 71). In the phytopathogen *R. fascians*, virulence is conferred by a
513 linear conjugative plasmid (45) without obvious similarity to pVAPN, illustrating that
514 multiple extrachromosomal elements serve as platforms for the expression and dynamic
515 exchange of niche-adaptive traits in the genus *Rhodococcus*.

516 Our findings suggest the following hypothetical scenario for the evolution of virulence
517 in *R. equi* (Fig. 6). First, acquisition of an ancestral *vap* PAI by a circular conjugative plasmid
518 endowed a “pre-*R. equi*” obligate saprotroph with intracellular survival capability in
519 macrophages, promoting its conversion into a facultative parasite. During co-evolution with
520 animal hosts, porcine- and equine-specific tropism evolved as a secondary trait of the PAI in
521 the circular plasmid (Fig. 6B), involving gene duplication and sequence diversification within
522 the *vap* multigene family (Fig. 6A). Finally, acquisition of the *vap* PAI by a linear plasmid,
523 presumably from a direct precursor of the equine pVAPA (Fig. 6B), gave rise to the bovine-
524 adapted pVAPN in which another set of specific *vap* genes evolved (Fig. 6A).

525 Our analyses with pVAPN confirm the notion that the primary function of the *R. equi*
526 virulence plasmids is to support intracellular proliferation in macrophages. This primordial
527 function is clearly dissociable from host tropism, since epidemiological or experimental
528 evidence indicates that *R. equi* plasmids promote virulence in accidental (non-adapted) animal
529 hosts, such as humans or mice, regardless of their species-specific type. Our data indicate that
530 a specific *vap* gene, which was present in the nearest common ancestor of the contemporary
531 PAIs and evolved into the allelic variants *vapA* in pVAPA and *vapN* in pVAPN (and possibly
532 *vapB* in the porcine pVAPB), is critical for intracellular survival in macrophages.

533 Why bovine host tropism evolved in a linear replicon and not by further host-driven
534 diversification of the PAI in the circular pVAP replicon remains unclear. Since pVAPA and
535 pVAPB share a virtually identical circular backbone, equine- and porcine-specific infectivity

536 most likely resides in their divergent *vap* PAI. Whether determinants outside the *vap* PAI in
537 the unrelated pVAPN backbone contribute adaptive features which optimize the interaction of
538 *R. equi* with the bovine host requires further investigation.

539 The findings in this study establish *R. equi* as a novel paradigm of multihost-adapted
540 pathogen. The pVAPN plasmid here reported, together with the previously characterized
541 equine- and porcine-associated plasmids, provide a unique model system to gain a better
542 understanding of the bacterial mechanisms of intramacrophage survival and host tropism.

543

544 **ACKNOWLEDGEMENTS**

545 We thank F. Quigley and C. Lämmle for providing the bovine isolates the pVAPN plasmid
546 was sequenced from, M. Letek for his early contributions to the *R. equi* genome program, J.
547 Navas for initial help with mating experiments, P. Iglesias for technical assistance, and U.
548 Fogarty and colleagues at the Irish Equine Centre for their support. We also thank Edinburgh
549 Genomics (<http://genomics.ed.ac.uk/>) for pVAP1571 plasmid DNA sequencing and
550 preliminary read assembly.

551 This work was supported by the Horserace Betting Levy Board (grants vet/prj/712 and
552 753 to JV-B) and partially by the Research Stimulus Fund (grant RSF 06 379 to JV-B and
553 WM) and core BBSRC funding from the Roslin Institute. AV-R was supported by an EU
554 Marie-Curie postdoctoral fellowship, AH and EA by BBSRC-funded PhD studentships from
555 the Centre for Infectious Diseases of the University of Edinburgh (UoE), and IM by a Charles
556 Darwin international scholarship from UoE.

557 REFERENCES

- 558 1. **Prescott JF.** 1991. *Rhodococcus equi*: an animal and human pathogen. Clin Microbiol
559 Rev 4:20-34.
- 560 2. **Vazquez-Boland JA, Giguère S, Hapeshi A, MacArthur I, Anastasi E, Valero-Rello**
561 **A.** 2013. *Rhodococcus equi*: the many facets of a pathogenic actinomycete. Vet
562 Microbiol 167:9-33.
- 563 3. **Muscatello G, Leadon DP, Klayt M, Ocampo-Sosa A, Lewis DA, Fogarty U,**
564 **Buckley T, Gilkerson JR, Meijer WG, Vazquez-Boland JA.** 2007. *Rhodococcus equi*
565 infection in foals: the science of 'rattles'. Equine Vet J 39:470-478.
- 566 4. **Cohen ND, Chaffin MK, Kuskie KR, Syndergaard MK, Blodgett GP, Takai S.**
567 2013. Association of perinatal exposure to airborne *Rhodococcus equi* with risk of
568 pneumonia caused by *R. equi* in foals. Am J Vet Res 74:102-109.
- 569 5. **Giguère S, Cohen ND, Chaffin MK, Hines SA, Hondalus MK, Prescott JF, Slovis**
570 **NM.** 2011. *Rhodococcus equi*: clinical manifestations, virulence, and immunity. J Vet
571 Intern Med 25:1221-1230.
- 572 6. **Kinne J, Madarame H, Takai S, Jose S, Wernery U.** 2011. Disseminated
573 *Rhodococcus equi* infection in dromedary camels (*Camelus dromedarius*). Vet
574 Microbiol 149:269-272.
- 575 7. **Takai S, Martens RJ, Julian A, Garcia Ribeiro M, Rodrigues de Farias M, Sasaki**
576 **Y, Inuzuka K, Kakuda T, Tsubaki S, Prescott JF.** 2003. Virulence of *Rhodococcus*
577 *equi* isolated from cats and dogs. J Clin Microbiol 41:4468-4470.
- 578 8. **Weinstock DM, Brown AE.** 2002. *Rhodococcus equi*: an emerging pathogen. Clin
579 Infect Dis 34:1379-1385.
- 580 9. **Takai S, Fukunaga N, Ochiai S, Imai Y, Sasaki Y, Tsubaki S, Sekizaki T.** 1996.
581 Identification of intermediately virulent *Rhodococcus equi* isolates from pigs. J Clin
582 Microbiol 34:1034-1037.
- 583 10. **Makrai L, Takayama S, Denes B, Hajtos I, Sasaki Y, Kakuda T, Tsubaki S, Major**
584 **A, Fodor L, Varga J, Takai S.** 2005. Characterization of virulence plasmids and
585 serotyping of *Rhodococcus equi* isolates from submaxillary lymph nodes of pigs in
586 Hungary. J Clin Microbiol 43:1246-1250.
- 587 11. **Komijn RE, Wisselink HJ, Rijsman VM, Stockhofe-Zurwieden N, Bakker D, van**
588 **Zijderveld FG, Eger T, Wagenaar JA, Putirulan FF, Urlings BA.** 2007.
589 Granulomatous lesions in lymph nodes of slaughter pigs bacteriologically negative for
590 *Mycobacterium avium* subsp. *avium* and positive for *Rhodococcus equi*. Vet Microbiol
591 120:352-357.
- 592 12. **Flynn O, Quigley F, Costello E, O'Grady D, Gogarty A, Mc Guirk J, Takai S.** 2001.
593 Virulence-associated protein characterisation of *Rhodococcus equi* isolated from bovine
594 lymph nodes. Vet Microbiol 78:221-228.
- 595 13. **Torres-Tortosa M, Arrizabalaga J, Villanueva JL, Galvez J, Leyes M, Valencia**
596 **ME, Flores J, Pena JM, Perez-Cecilia E, Quereda C.** 2003. Prognosis and clinical
597 evaluation of infection caused by *Rhodococcus equi* in HIV-infected patients: a
598 multicenter study of 67 cases. Chest 123:1970-1976.
- 599 14. **Kedlaya I, Ing MB, Wong SS.** 2001. *Rhodococcus equi* infections in
600 immunocompetent hosts: case report and review. Clin Infect Dis 32:E39-46.

- 601 15. **Hondalus MK, Mosser DM.** 1994. Survival and replication of *Rhodococcus equi* in
602 macrophages. *Infect Immun* **62**:4167-4175.
- 603 16. **Toyooka K, Takai S, Kirikae T.** 2005. *Rhodococcus equi* can survive a
604 phagolysosomal environment in macrophages by suppressing acidification of the
605 phagolysosome. *J Med Microbiol* **54**:1007-1015.
- 606 17. **Zink MC, Yager JA, Prescott JF, Fernando MA.** 1987. Electron microscopic
607 investigation of intracellular events after ingestion of *Rhodococcus equi* by foal alveolar
608 macrophages. *Vet Microbiol* **14**:295-305.
- 609 18. **von Bargen K, Haas A.** 2009. Molecular and infection biology of the horse pathogen
610 *Rhodococcus equi*. *FEMS Microbiol Rev* **33**:870-891.
- 611 19. **Takai S, Watanabe Y, Ikeda T, Ozawa T, Matsukura S, Tamada Y, Tsubaki S,**
612 **Sekizaki T.** 1993. Virulence-associated plasmids in *Rhodococcus equi*. *J Clin Microbiol*
613 **31**:1726-1729.
- 614 20. **Takai S, Hines SA, Sekizaki T, Nicholson VM, Alperin DA, Osaki M, Takamatsu**
615 **D, Nakamura M, Suzuki K, Ogino N, Kakuda T, Dan H, Prescott JF.** 2000. DNA
616 sequence and comparison of virulence plasmids from *Rhodococcus equi* ATCC 33701
617 and 103. *Infect Immun* **68**:6840-6847.
- 618 21. **Giguère S, Hondalus MK, Yager JA, Darrah P, Mosser DM, Prescott JF.** 1999.
619 Role of the 85-kilobase plasmid and plasmid-encoded virulence-associated protein A in
620 intracellular survival and virulence of *Rhodococcus equi*. *Infect Immun* **67**:3548-3557.
- 621 22. **Fernandez-Mora E, Polidori M, Luhrmann A, Schaible UE, Haas A.** 2005.
622 Maturation of *Rhodococcus equi*-containing vacuoles is arrested after completion of the
623 early endosome stage. *Traffic* **6**:635-653.
- 624 23. **Coulson GB, Agarwal S, Hondalus MK.** 2010. Characterization of the role of the
625 pathogenicity island and *vapG* in the virulence of the intracellular actinomycete
626 pathogen *Rhodococcus equi*. *Infect Immun* **78**:3323-3334.
- 627 24. **Letek M, Ocampo-Sosa AA, Sanders M, Fogarty U, Buckley T, Leadon DP,**
628 **Gonzalez P, Scortti M, Meijer WG, Parkhill J, Bentley S, Vazquez-Boland JA.**
629 2008. Evolution of the *Rhodococcus equi vap* pathogenicity island seen through
630 comparison of host-associated *vapA* and *vapB* virulence plasmids. *J Bacteriol* **190**:5797-
631 5805.
- 632 25. **Byrne BA, Prescott JF, Palmer GH, Takai S, Nicholson VM, Alperin DC, Hines**
633 **SA.** 2001. Virulence plasmid of *Rhodococcus equi* contains inducible gene family
634 encoding secreted proteins. *Infect Immun* **69**:650-656.
- 635 26. **Jain S, Bloom BR, Hondalus MK.** 2003. Deletion of *vapA* encoding Virulence
636 Associated Protein A attenuates the intracellular actinomycete *Rhodococcus equi*. *Mol*
637 *Microbiol* **50**:115-128.
- 638 27. **Gonzalez-Iglesias P, Scortti M, MacArthur I, Hapeshi A, Rodriguez H, Prescott**
639 **JF, Vazquez-Boland JA.** 2014. Mouse lung infection model to assess *Rhodococcus*
640 *equi* virulence and vaccine protection. *Vet Microbiol* **172**:256-264.
- 641 28. **Takai S, Sekizaki T, Ozawa T, Sugawara T, Watanabe Y, Tsubaki S.** 1991.
642 Association between a large plasmid and 15- to 17-kilodalton antigens in virulent
643 *Rhodococcus equi*. *Infect Immun* **59**:4056-4060.
- 644 29. **Sekizaki T, Takai S, Egawa Y, Ikeda T, Ito H, Tsubaki S.** 1995. Sequence of the
645 *Rhodococcus equi* gene encoding the virulence-associated 15-17-kDa antigens. *Gene*
646 **155**:135-136.

- 647 30. **Takai S, Anzai T, Fujita Y, Akita O, Shoda M, Tsubaki S, Wada R.** 2000.
648 Pathogenicity of *Rhodococcus equi* expressing a virulence-associated 20 kDa protein
649 (VapB) in foals. *Vet Microbiol* **76**:71-80.
- 650 31. **Oldfield C, Bonella H, Renwick L, Dodson HI, Alderson G, Goodfellow M.** 2004.
651 Rapid determination of *vapA/vapB* genotype in *Rhodococcus equi* using a differential
652 polymerase chain reaction method. *A Van Leeuw J Microb* **85**:317-326.
- 653 32. **Makrai L, Takai S, Tamura M, Tsukamoto A, Sekimoto R, Sasaki Y, Kakuda T,**
654 **Tsubaki S, Varga J, Fodor L, Solymosi N, Major A.** 2002. Characterization of
655 virulence plasmid types in *Rhodococcus equi* isolates from foals, pigs, humans and soil
656 in Hungary. *Vet Microbiol* **88**:377-384.
- 657 33. **Takai S, Tharavichitkul P, Takarn P, Khantawa B, Tamura M, Tsukamoto A,**
658 **Takayama S, Yamatoda N, Kimura A, Sasaki Y, Kakuda T, Tsubaki S,**
659 **Maneekarn N, Sirisanthana T, Kirikae T.** 2003. Molecular epidemiology of
660 *Rhodococcus equi* of intermediate virulence isolated from patients with and without
661 acquired immune deficiency syndrome in Chiang Mai, Thailand. *J Infect Dis* **188**:1717-
662 1723.
- 663 34. **Ocampo-Sosa AA, Lewis DA, Navas J, Quigley F, Callejo R, Scotti M, Leadon**
664 **DP, Fogarty U, Vazquez-Boland JA.** 2007. Molecular epidemiology of *Rhodococcus*
665 *equi* based on *traA*, *vapA*, and *vapB* virulence plasmid markers. *J Infect Dis* **196**:763-
666 769.
- 667 35. **Soedarmanto I, Oliveira R, Lämmler C, Durrling H.** 1997. Identification and
668 epidemiological relationship of *Rhodococcus equi* isolated from cases of lymphadenitis
669 in cattle. *Zentralbl Bakteriell* **286**:457-467.
- 670 36. **Navas J, Gonzalez-Zorn B, Ladron N, Garrido P, Vazquez-Boland JA.** 2001.
671 Identification and mutagenesis by allelic exchange of *choE*, encoding a cholesterol
672 oxidase from the intracellular pathogen *Rhodococcus equi*. *J Bacteriol* **183**:4796-4805.
- 673 37. **McLeod MP, Warren RL, Hsiao WW, Araki N, Myhre M, Fernandes C,**
674 **Miyazawa D, Wong W, Lillquist AL, Wang D, Dosanjh M, Hara H, Petrescu A,**
675 **Morin RD, Yang G, Stott JM, Schein JE, Shin H, Smailus D, Siddiqui AS, Marra**
676 **MA, Jones SJ, Holt R, Brinkman FS, Miyauchi K, Fukuda M, Davies JE, Mohn**
677 **WW, Eltis LD.** 2006. The complete genome of *Rhodococcus* sp. RHA1 provides
678 insights into a catabolic powerhouse. *Proc Natl Acad Sci U S A* **103**:15582-15587.
- 679 38. **van der Geize R, de Jong W, Hessels GI, Grommen AW, Jacobs AA, Dijkhuizen L.**
680 2008. A novel method to generate unmarked gene deletions in the intracellular pathogen
681 *Rhodococcus equi* using 5-fluorocytosine conditional lethality. *Nucleic Acids Res*
682 **36**:e151.
- 683 39. **Tripathi VN, Harding WC, Willingham-Lane JM, Hondalus MK.** 2012. Conjugal
684 transfer of a virulence plasmid in the opportunistic intracellular actinomycete
685 *Rhodococcus equi*. *J Bacteriol* **194**:6790-6801.
- 686 40. **Letek M, Gonzalez P, Macarthur I, Rodriguez H, Freeman TC, Valero-Rello A,**
687 **Blanco M, Buckley T, Cherevach I, Fahey R, Hapeshi A, Holdstock J, Leadon D,**
688 **Navas J, Ocampo A, Quail MA, Sanders M, Scotti MM, Prescott JF, Fogarty U,**
689 **Meijer WG, Parkhill J, Bentley SD, Vazquez-Boland JA.** 2010. The genome of a
690 pathogenic *Rhodococcus*: cooptive virulence underpinned by key gene acquisitions.
691 *PLoS Genet* **6**:e1001145.
- 692 41. **Deshayes C, Bielecka MK, Cain RJ, Scotti M, de las Heras A, Pietras Z, Luisi BF,**
693 **Nunez Miguel R, Vazquez-Boland JA.** 2012. Allosteric mutants show that PrfA

- activation is dispensable for vacuole escape but required for efficient spread and *Listeria* survival *in vivo*. *Mol Microbiol* **85**:461-477.
42. **Shimizu S, Kobayashi H, Masai E, Fukuda M.** 2001. Characterization of the 450-kb linear plasmid in a polychlorinated biphenyl degrader, *Rhodococcus* sp. strain RHA1. *Appl Environ Microbiol* **67**:2021-2028.
 43. **Zhang R, Yang Y, Fang P, Jiang C, Xu L, Zhu Y, Shen M, Xia H, Zhao J, Chen T, Qin Z.** 2006. Diversity of telomere palindromic sequences and replication genes among *Streptomyces* linear plasmids. *Appl Environ Microbiol* **72**:5728-5733.
 44. **Sekine M, Tanikawa S, Omata S, Saito M, Fujisawa T, Tsukatani N, Tajima T, Sekigawa T, Kosugi H, Matsuo Y, Nishiko R, Imamura K, Ito M, Narita H, Tago S, Fujita N, Harayama S.** 2006. Sequence analysis of three plasmids harboured in *Rhodococcus erythropolis* strain PR4. *Environ Microbiol* **8**:334-346.
 45. **Francis I, De Keyser A, De Backer P, Simon-Mateo C, Kalkus J, Pertry I, Ardiles-Diaz W, De Rycke R, Vandeputte OM, El Jaziri M, Holsters M, Vereecke D.** 2012. pFiD188, the linear virulence plasmid of *Rhodococcus fascians* D188. *Mol Plant Microb In* **25**:637-647.
 46. **Larkin MJ, Kulakov LA, Allen CCR.** 2010. Genomes and plasmids in *Rhodococcus*, p 73-90. In Alvarez HM (ed), *Biology of Rhodococcus*. Springer.
 47. **Stecker C, Johann A, Herzberg C, Averhoff B, Gottschalk G.** 2003. Complete nucleotide sequence and genetic organization of the 210-kilobase linear plasmid of *Rhodococcus erythropolis* BD2. *J Bacteriol* **185**:5269-5274.
 48. **Zhu Y, Xu M, Shen M, Chen Z, Qin Z.** 2010. [Cloning, sequencing and identification of replication origin of *Rhodococcus* linear plasmid pNSL1]. *Wei Sheng Wu Xue Bao = Acta Microbiologica Sinica* **50**:1098-1103.
 49. **Garcillan-Barcia MP, Francia MV, de la Cruz F.** 2009. The diversity of conjugative relaxases and its application in plasmid classification. *FEMS Microbiol Rev* **33**:657-687.
 50. **de la Cruz F, Frost LS, Meyer RJ, Zechner EL.** 2010. Conjugative DNA metabolism in Gram-negative bacteria. *FEMS Microbiol Rev* **34**:18-40.
 51. **Guglielmini J, de la Cruz F, Rocha EP.** 2013. Evolution of conjugation and type IV secretion systems. *Mol Biol Evol* **30**:315-331.
 52. **Vernikos GS, Parkhill J.** 2006. Interpolated variable order motifs for identification of horizontally acquired DNA: revisiting the *Salmonella* pathogenicity islands. *Bioinformatics* **22**:2196-2203.
 53. **Vogelmann J, Ammelburg M, Finger C, Guezguez J, Linke D, Flotenmeyer M, Stierhof YD, Wohlleben W, Muth G.** 2011. Conjugal plasmid transfer in *Streptomyces* resembles bacterial chromosome segregation by FtsK/SpoIIIE. *EMBO J* **30**:2246-2254.
 54. **Ebersbach G, Gerdes K.** 2005. Plasmid segregation mechanisms. *Annu Rev Genet* **39**:453-479.
 55. **Atmakuri K, Cascales E, Burton OT, Banta LM, Christie PJ.** 2007. *Agrobacterium* ParA/MinD-like VirC1 spatially coordinates early conjugative DNA transfer reactions. *EMBO J* **26**:2540-2551.
 56. **Schue M, Maurin D, Dhouib R, Bakala N'Goma JC, Delorme V, Lambeau G, Carriere F, Canaan S.** 2010. Two cutinase-like proteins secreted by *Mycobacterium tuberculosis* show very different lipolytic activities reflecting their physiological function. *FASEB J* **24**:1893-1903.

- 740 57. **West NP, Chow FM, Randall EJ, Wu J, Chen J, Ribeiro JM, Britton WJ.** 2009.
741 Cutinase-like proteins of *Mycobacterium tuberculosis*: characterization of their variable
742 enzymatic functions and active site identification. *FASEB J* **23**:1694-1704.
- 743 58. **Parker SK, Curtin KM, Vasil ML.** 2007. Purification and characterization of
744 mycobacterial phospholipase A: an activity associated with mycobacterial cutinase. *J*
745 *Bacteriol* **189**:4153-4160.
- 746 59. **Salifu SP, Valero-Rello A, Campbell SA, Inglis NF, Scortti M, Foley S, Vazquez-**
747 **Boland JA.** 2013. Genome and proteome analysis of phage E3 infecting the soil-borne
748 actinomycete *Rhodococcus equi*. *Environ Microbiol Rep* **5**:170-178.
- 749 60. **Schumacher MA, Funnell BE.** 2005. Structures of ParB bound to DNA reveal
750 mechanism of partition complex formation. *Nature* **438**:516-519.
- 751 61. **Ren J, Prescott JF.** 2004. The effect of mutation on *Rhodococcus equi* virulence
752 plasmid gene expression and mouse virulence. *Vet Microbiol* **103**:219-230.
- 753 62. **Russell DA, Byrne GA, O'Connell EP, Boland CA, Meijer WG.** 2004. The LysR-
754 type transcriptional regulator VirR is required for expression of the virulence gene *vapA*
755 of *Rhodococcus equi* ATCC 33701. *J Bacteriol* **186**:5576-5584.
- 756 63. **Wang X, Coulson GB, Miranda-Casoluengo AA, Miranda-Casoluengo R,**
757 **Hondalus MK, Meijer WG.** 2014. IcgA is a virulence factor of *Rhodococcus equi* that
758 modulates intracellular growth. *Infect Immun* **82**:1793-1800.
- 759 64. **Chen JM, German GJ, Alexander DC, Ren H, Tan T, Liu J.** 2006. Roles of Lsr2 in
760 colony morphology and biofilm formation of *Mycobacterium smegmatis*. *J Bacteriol*
761 **188**:633-641.
- 762 65. **Colangeli R, Haq A, Arcus VL, Summers E, Magliozzo RS, McBride A, Mitra AK,**
763 **Radjainia M, Khajo A, Jacobs WR, Jr., Salgame P, Alland D.** 2009. The
764 multifunctional histone-like protein Lsr2 protects mycobacteria against reactive oxygen
765 intermediates. *Proc Natl Acad Sci U S A* **106**:4414-4418.
- 766 66. **Bartek IL, Woolhiser LK, Baughn AD, Basaraba RJ, Jacobs WR, Jr., Lenaerts AJ,**
767 **Voskuil MI.** 2014. *Mycobacterium tuberculosis* Lsr2 is a global transcriptional
768 regulator required for adaptation to changing oxygen levels and virulence. *mBio*
769 **5**:e01106-01114.
- 770 67. **Miranda-Casoluengo R, Miranda-Casoluengo AA, O'Connell EP, Fahey RJ,**
771 **Boland CA, Vazquez-Boland JA, Meijer WG.** 2011. The *vapA* co-expressed
772 virulence plasmid gene *vcgB* (*orf10*) of the intracellular actinomycete *Rhodococcus*
773 *equi*. *Microbiol* **157**:2357-2368.
- 774 66. **Durand D, Halldorsson BV, Vernot B.** 2006. A hybrid micro-macroevolutionary
775 approach to gene tree reconstruction. *J Comput Biol* **13**:320-335.
- 776 69. **Chiang SL, Mekalanos JJ, Holden DW.** 1999. *In vivo* genetic analysis of bacterial
777 virulence. *Annu Rev Microbiol* **53**:129-154.
- 778 70. **Beuzon CR, Holden DW.** 2001. Use of mixed infections with *Salmonella* strains to
779 study virulence genes and their interactions *in vivo*. *Microb Infect* **3**:1345-1352.
- 780 71. **Larkin MJ, Kulakov LA, Allen CC.** 2005. Biodegradation and *Rhodococcus*--masters
781 of catabolic versatility. *Curr Opin Biotechnol* **16**:282-290.
- 782 72. **Bao K, Cohen SN.** 2003. Recruitment of terminal protein to the ends of *Streptomyces*
783 linear plasmids and chromosomes by a novel telomere-binding protein essential for
784 linear DNA replication. *Genes Dev* **17**:774-785.

785

786 **Table 1.** Competitive indexes (C.I.) of Fig. 8 experiments. Mean values \pm SEM. A C.I. equal to
787 1 is the theoretical value of two strains with the same competitive ability. Data significance was
788 calculated by comparing the experimental C.I. value at each time point against the theoretical
789 value 1 (one sample Student's t test).
790

Competing strains	C.I. (<i>P</i> value)				
	day 0	day 1	day 2	day 3	day 4
1571 ⁻ / 1571	1.54 \pm 0.20 (.0763)	0.42 \pm 0.13 (.0225)	0.40 \pm 0.12 (.0407)	0.06 \pm 0.06 (.0051)	0.0 (.0001)
$\Delta vapN$ / 1571 ⁻	0.88 \pm 0.13 (.4761)	2.24 \pm 0.16 (.0049)	3.36 \pm 0.41 (.0107)	1.47 \pm 0.09 (.0363)	2.68 \pm 0.64 (.1197)

791

792 **FIGURE LEGENDS**

793

794 **FIG 1.** Detection of pVAPN by PFGE. (A) Genomic DNA of bovine isolate 1571 and equine
 795 isolate 103S; three and two independent lysates per strain are shown. Relevant positions of
 796 the lambda PFGE marker (New England Biolabs) are indicated. pVAPN is observable as a
 797 distinct PFGE band of ≈ 100 Kb in the bovine isolate. (B) Southern blot analysis of bovine
 798 isolates PAM nos. 1571, 1533 and 1554 (strain 103S used as negative control). Left, relevant
 799 sections of PFGE gel; right, membrane hybridized with a pVAPN-specific DNA probe (600
 800 bp fragment encompassing the 3' region of *vapN* and 5' region of *vapQ*). Arrow indicates the
 801 pVAPN band.

802

803 **FIG 2.** Plasmid genome alignments. Linear pVAPN, circular pVAPA and pVAPB, and
 804 respective closest homologs from non-pathogenic rhodococcal species (pNSL1 from
 805 *Rhodococcus* sp. NS1 (48) and pREC1 from *R. erythropolis* (44)). Built with EASYFIG
 806 (<http://easyfig.sourceforge.net/>). The circular plasmids (pVAPA, pVAPB, pREC1) were
 807 linearized starting from the first conserved gene of the housekeeping backbone. Regions with
 808 significant similarity between plasmids are connected by gray stripes (tblastx, 0.1 e-value
 809 threshold); grayscale indicates percent similarity. ORFs are color coded according to
 810 predicted function: hypothetical protein (gray), conjugation or DNA
 811 replication/recombination/metabolism (red), DNA mobility genes (magenta), transcriptional
 812 regulators (blue), secreted proteins (dark green), membrane proteins (pale green), metabolic
 813 functions (yellow), *vap* family gene (black); pseudogenes (brown). Other features indicated:
 814 green and pale red bars below the genes, conjugation and replication/partitioning functional
 815 modules, respectively; dotted underline, HGT regions identified by ALIEN HUNTER (52);
 816 triangle, putative origin of replication. Relevant gene products are labelled with abbreviations.

817

818 **FIG 3.** Maximum Likelihood (ML) trees of (A) *Rhodococcus* plasmid backbones and (B) *R.*
819 *equi vap* multigene family. HKY+G evolutionary model. (A) Based on concatenated
820 alignment of orthologs from a selection of rhodococcal extrachromosomal replicons (total
821 7,802 nucleotides); genes used indicated by dots in Fig. 2. Values >50 for 100 bootstrap
822 replicates are indicated. Symbols: triangles, linear plasmids; circles, circular plasmids. (B)
823 *vap* family members derived from each of the predicted seven precursor *vap* genes in the
824 lowest common ancestor (LCA) of the extant pVAPA, pVAPB and pVAPN PAIs are
825 encircled within gray balloons.

826

827 **FIG 4.** pVAPN telomeric sequences. (A) ClustalΩ alignment of the left- and right-end 200
828 terminal nucleotides. Identical nucleotides are shaded (dark and light blue, purines and
829 pyrimidines, respectively). Inverted repeats are indicated above the sequence. In red, four
830 conserved palindromic sequences with the central motif GCTNCGC identified in the binding
831 site of telomere-associated proteins involved in *Streptomyces* linear plasmid replication (73).
832 Several of the GCTNCGC palindromic sequences are normally present in the telomeres of
833 rhodococcal linear plasmids (43-45) (Fig. S2). (B) Secondary structures potentially formed by
834 the palindromic sequences in pVAPN telomeres, as numbered in (A). Determined with
835 MFOLD. Free energy: left, $\Delta G = -33.84$ kcal/mol; right, $\Delta G = -37.95$ kcal/mol.

836

837 **FIG 5.** Genetic structure of the *vap* PAIs from pVAPN (15.1 Kb), pVAPA (21.5 Kb) and
838 pVAPB (15.9 Kb). Genes are color-coded according to functional category: *vap* family
839 (black), DNA conjugation/partitioning (red), DNA mobility/recombination (magenta),
840 transcriptional regulators (blue), other regulators (cyan), membrane proteins (green),
841 metabolic reactions (yellow). Orthologs are in the same color shade and linked by gray bands.
842 ORFs encoding hypothetical proteins are represented in light blue-gray, in white if outside the
843 PAI. White arrowheads point to the first and last genes of the consensus PAI. The *traA*

844 pseudogene/phage excisionase-*rep-copG* HGT cluster from the pVAPA backbone is boxed.
 845 The figure also schematizes the probable evolutionary relationships of the *vap* multigene
 846 family as inferred from the phylogenetic analyses (Figs. 3B, S4, S5) and PAI genetic
 847 structure; the model minimizes the number of *vap* gene loss events. Solid lines/arrows
 848 connect *vap* genes belonging to the same monophyletic group (thus likely representing allelic
 849 variants of a nearest common *vap* gene ancestor). Curved lines/arrows indicate *vap* gene
 850 duplications within a PAI. Crosses denote *vap* genes lost, asterisks indicate pseudogenes. Two
 851 alternative evolutionary paths are shown for *vapA-B-K1/2-N* (see legend to Fig. S5 for
 852 additional details). The black dots indicate the non-*vap* genes used for the MLSA analysis in
 853 Fig. S4B.

854
 855 **FIG 6.** Hypothetical reconstruction of *vap* PAI evolution. (A) Model of *vap* multigene family
 856 evolution. Lines indicate the evolutionary path of the *vap* genes between ancestral PAI
 857 lineages L0 to L0'', nearest common ancestor (LCA) and extant PAIs. Pre-pVAPA designates
 858 the hypothetical direct precursor of the current pVAPA PAI. Gene birth-duplication events
 859 are indicated by red squares, loss events by crosses, pseudogenes by asterisks and white
 860 rimming. (B) Fate of *vap* PAI in *R. equi* virulence plasmid evolution. (a) Acquisition by
 861 rhodococcal circular replicon of *vap* PAI ancestor conferring ability to colonize macrophages;
 862 (b) Mobilization of *vap* PAI from pre-pVAPA plasmid to rhodococcal linear replicon; (c)
 863 evolution of species-specificity.

864
 865 **FIG 7.** Intracellular proliferation experiments in murine (J774A.1) and human (THP-1)
 866 macrophages. Data expressed as normalized Intracellular Growth Coefficient (IGC; see
 867 Materials & Methods). Means of three duplicate experiments \pm SEM. Statistical significance
 868 analyzed by 2-way ANOVA; *P* values of Šidák post-hoc multiple comparisons at each time
 869 point are shown if ≤ 0.05 . (A) Plasmidless derivative and in-frame $\Delta vapN$ mutant of bovine

isolate 1571. Two-way ANOVA *P* values: J774A.1 = 0.0007, THP-1 = 0.0160. (B) Plasmidless derivative and in-frame $\Delta vapA$ mutant of equine isolate 103S. Two-way ANOVA *P* values: J774A.1 = 0.0112, THP-1 < 0.0001.

FIG 8. Competitive virulence assay in mouse lung. BALB/c mice (*n* = 4 per time point) were infected intranasally with a \approx 1:1 mixture of the test bacteria and the competing populations monitored 60 min after infection (*t* = 0) and then daily on four consecutive days. Bar height denotes total lung CFU and the light and dark grey areas within bars indicates the proportion of the competing bacteria. Corresponding competitive index (C.I.) are shown in Table 1. (A) Competition between wild-type bovine isolate 1571 and isogenic plasmidless derivative 1571⁻; infection dose: 3.7×10^7 CFU/mouse (2.3×10^7 and 1.4×10^7 , respectively). (B) Competition between the avirulent 1571⁻ strain and in-frame 1571 $\Delta vapN$ deletion mutant. Infection dose: 7.8×10^7 CFU/mouse (3.2×10^7 and 4.6×10^7 , respectively).

FIG 9. Transfer of pVAPN by mating confers virulence to a plasmid-negative *R. equi* recipient strain. (A) *In vivo* selection of pVAPN transconjugants in mice. Note the progressive enrichment of the recipient 103S^{-RmpR} strain upon acquisition of the pVAPN plasmid. *t* = 0, 60 min after infection. (B) Intracellular proliferation in J774A.1 macrophages. Acquisition of pVAPN (and the control pVAPA) plasmid promotes intracellular proliferation to the recipient 103S^{-RmpR} strain. Data expressed as normalized Intracellular Growth Coefficient (IGC; see Materials & Methods). Mean of three duplicate experiments \pm SEM; *P* values (2-way ANOVA, Šidák post-hoc multiple comparison) are indicated.

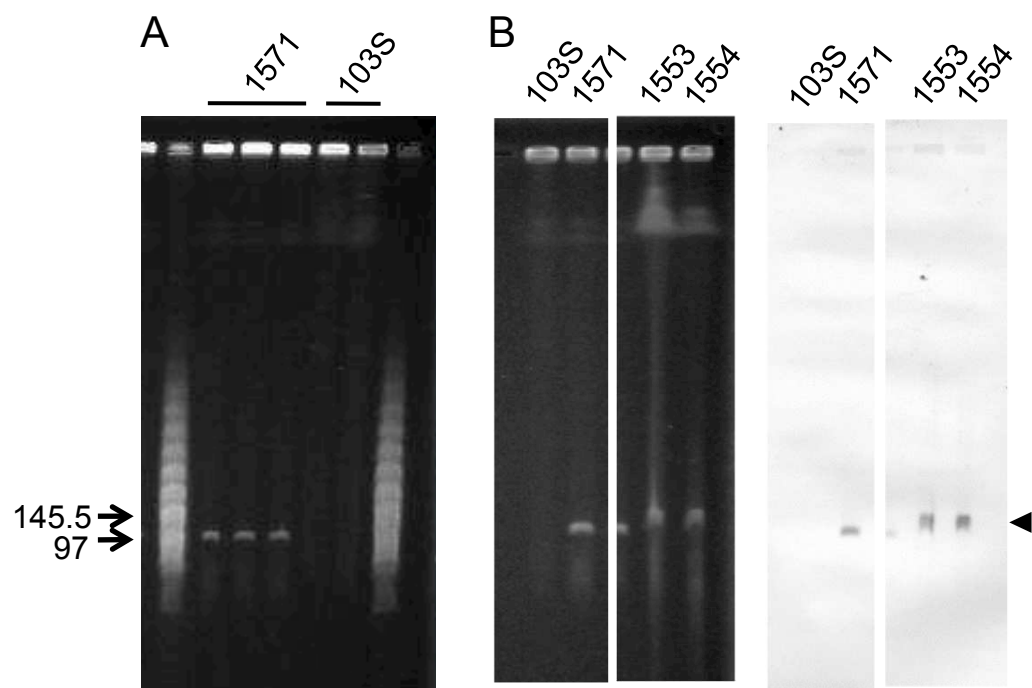


Fig. 1

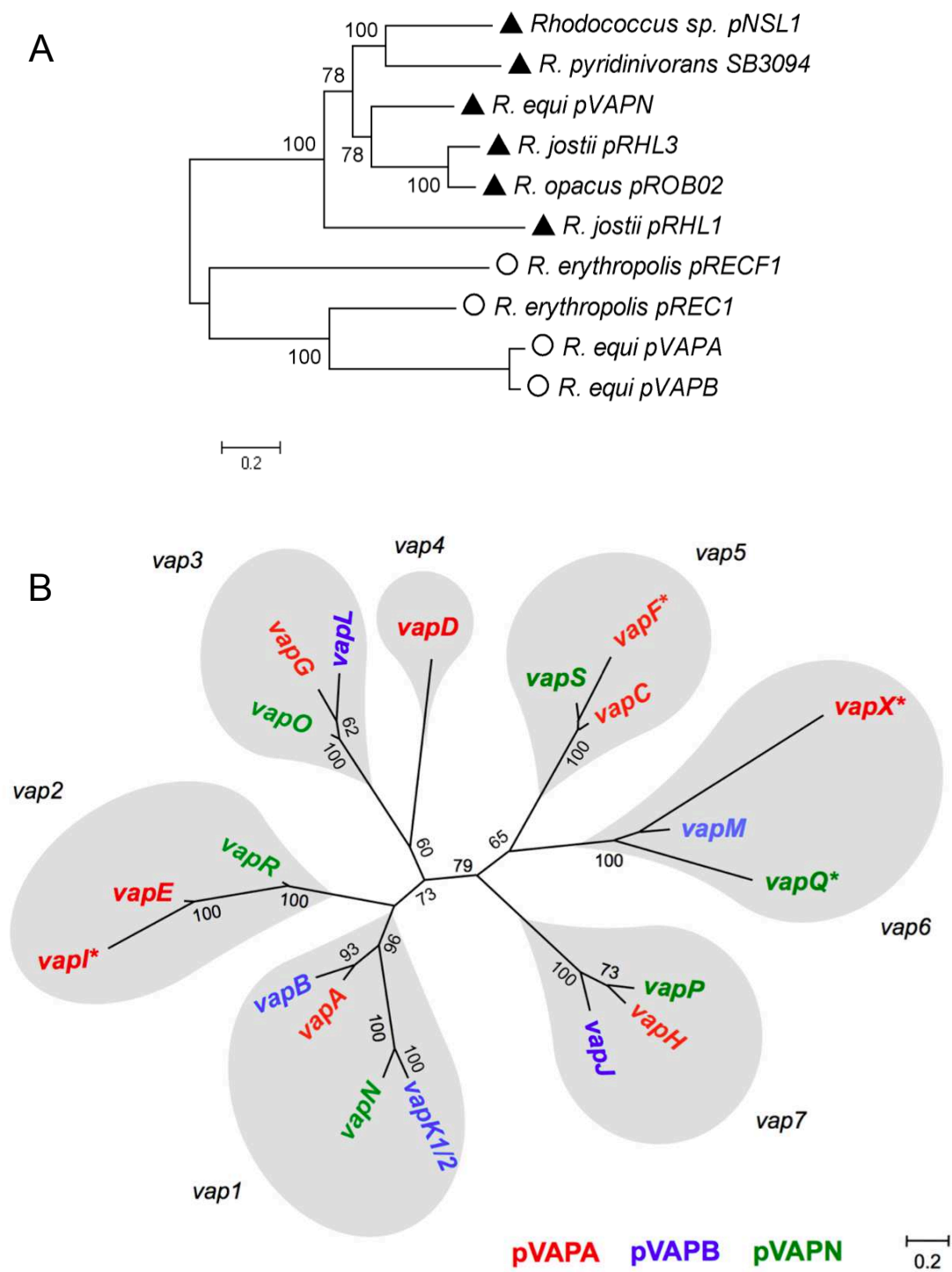


Fig. 3

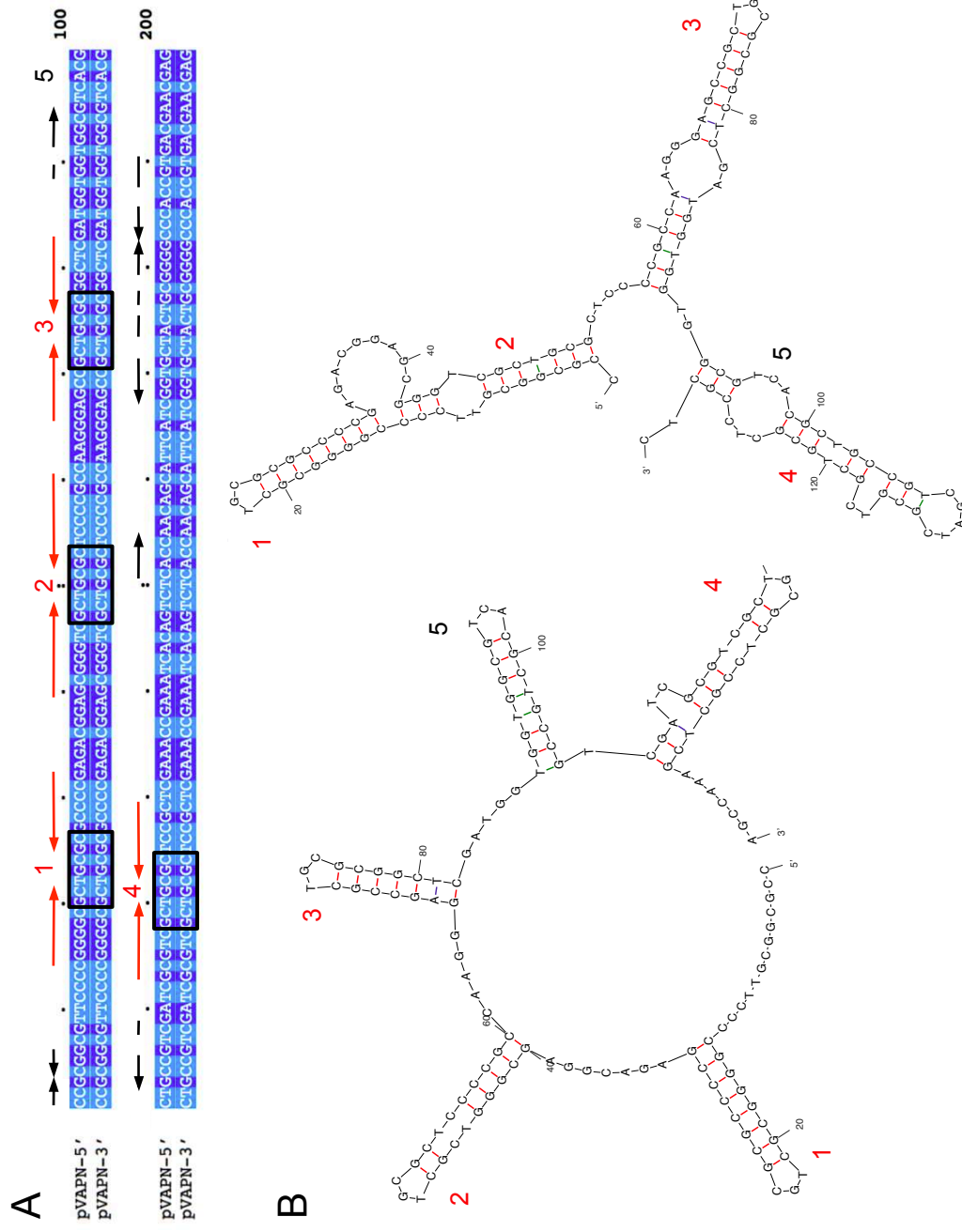
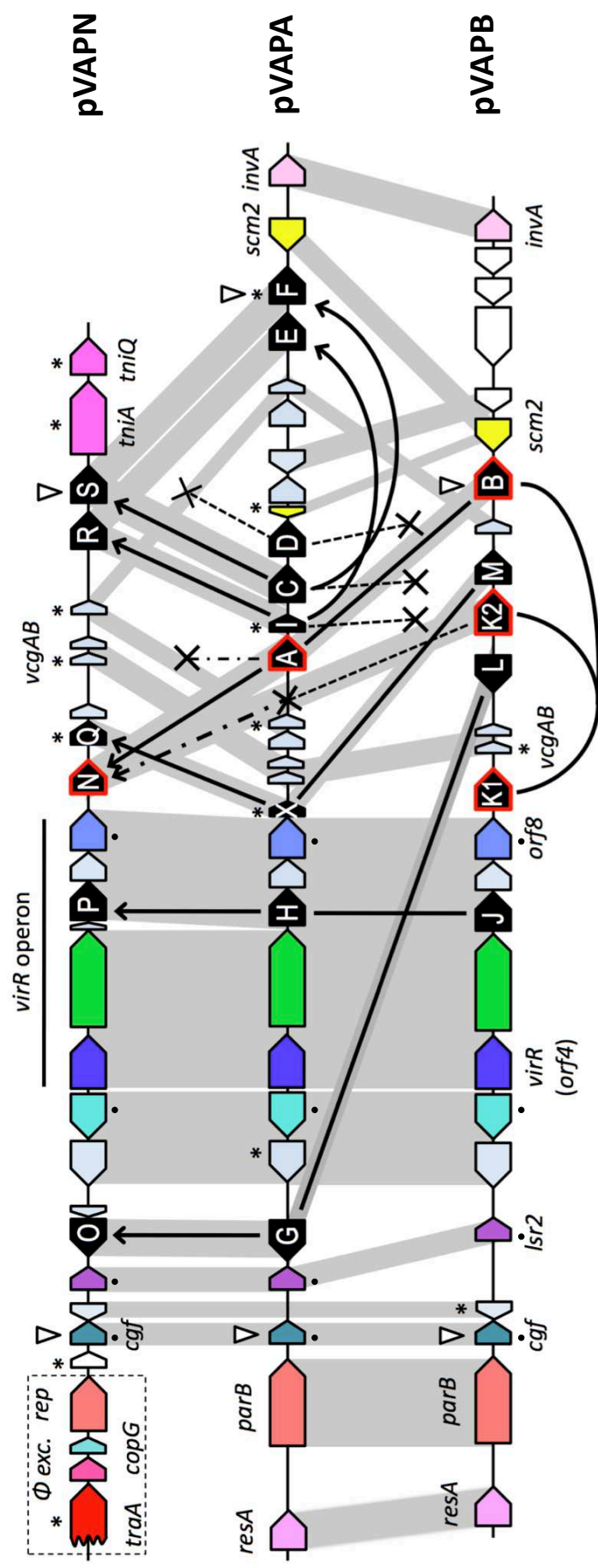


Fig. 4



Fi. 5

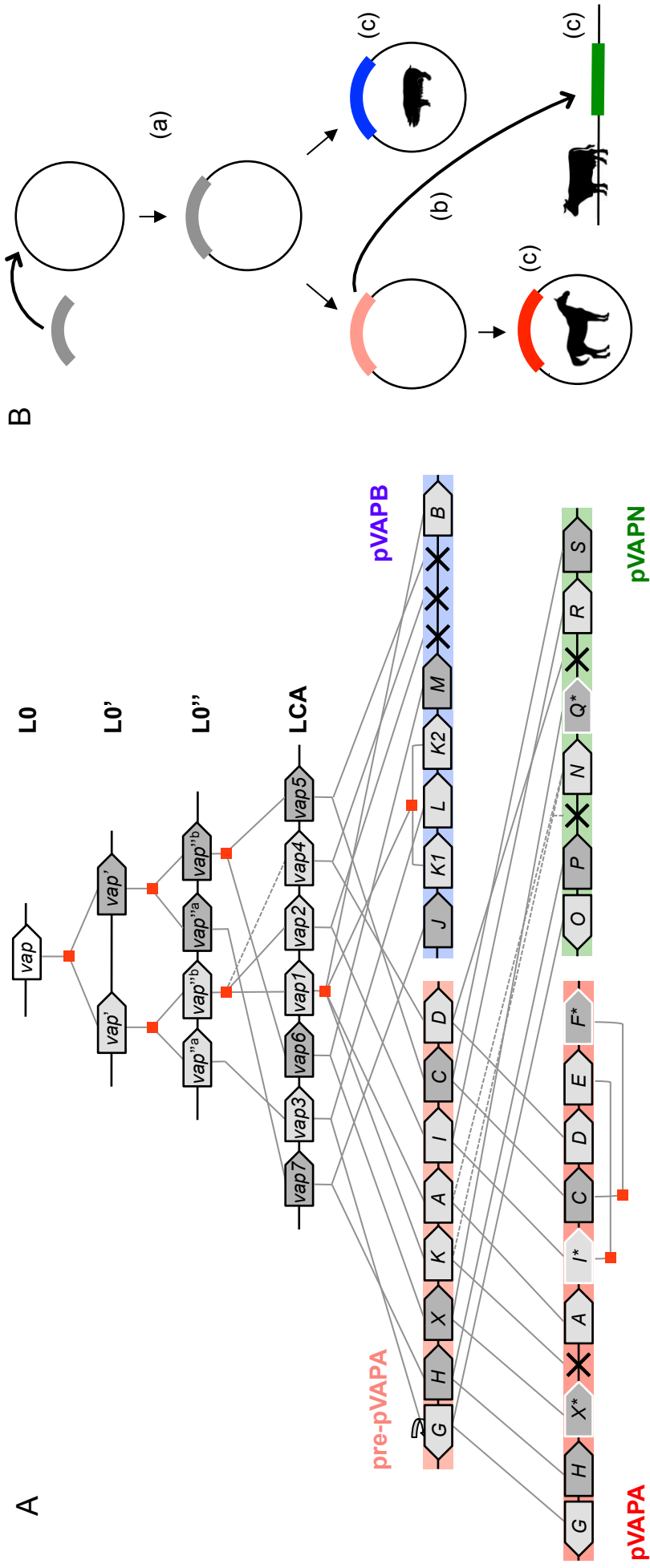


Fig. 6

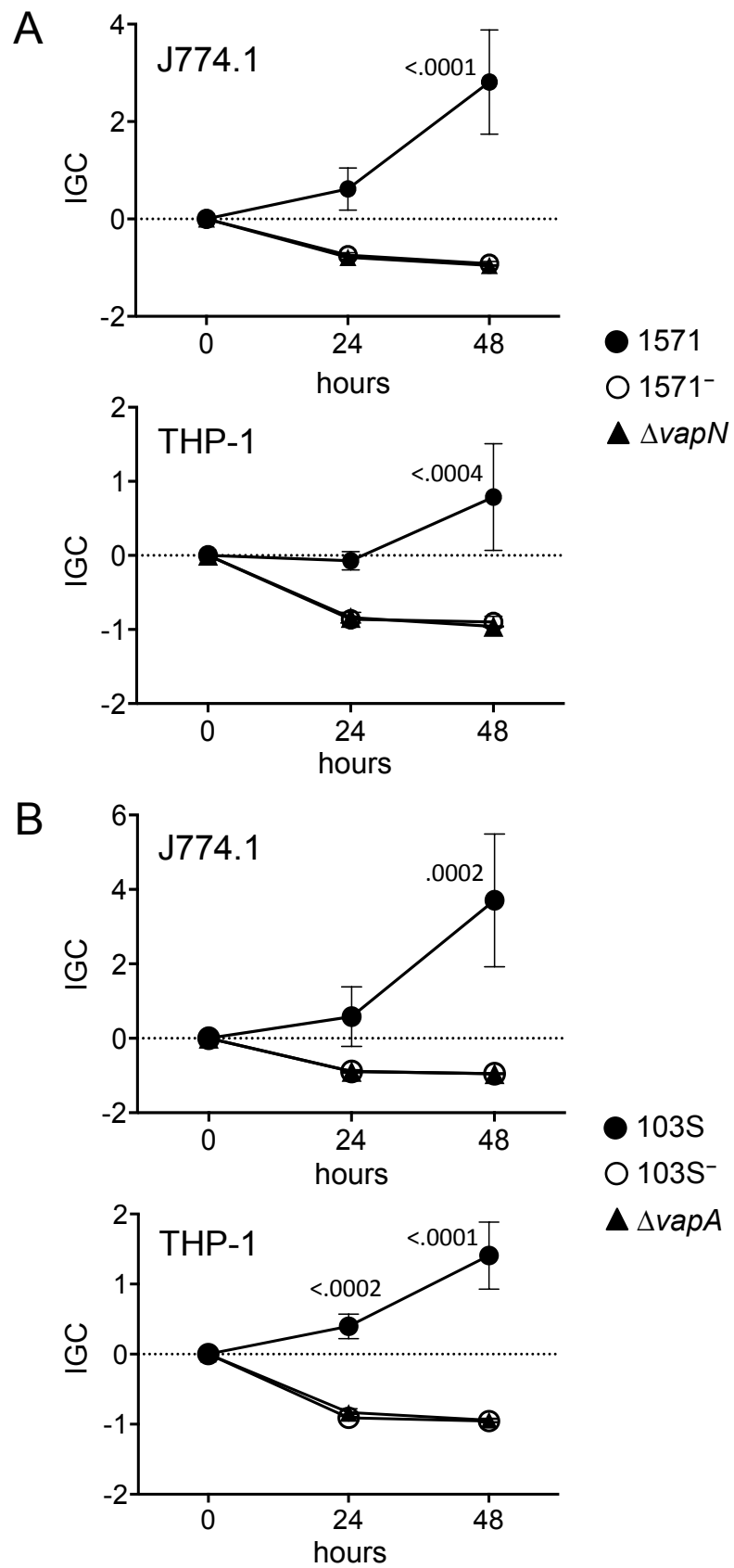


Fig. 7

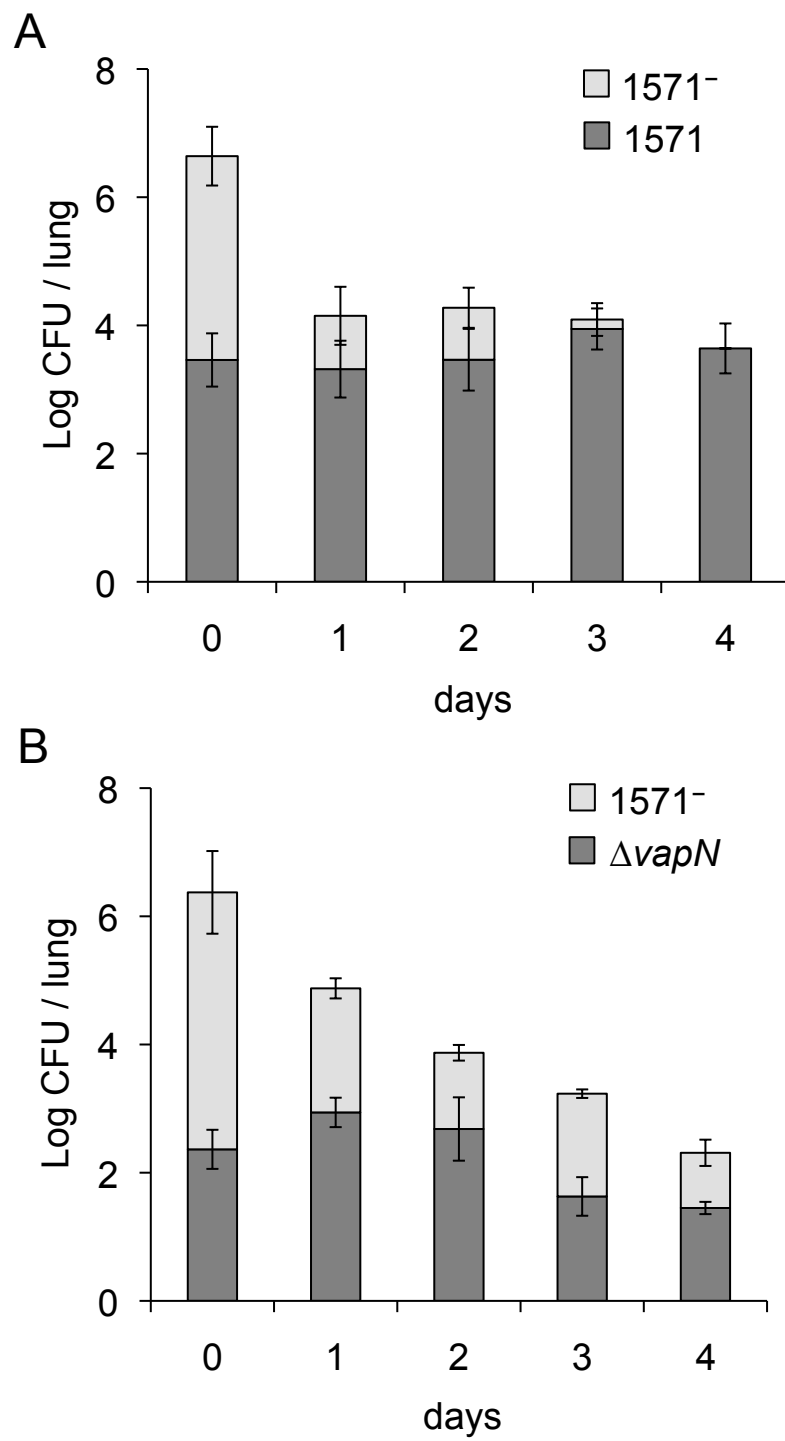


Fig. 8

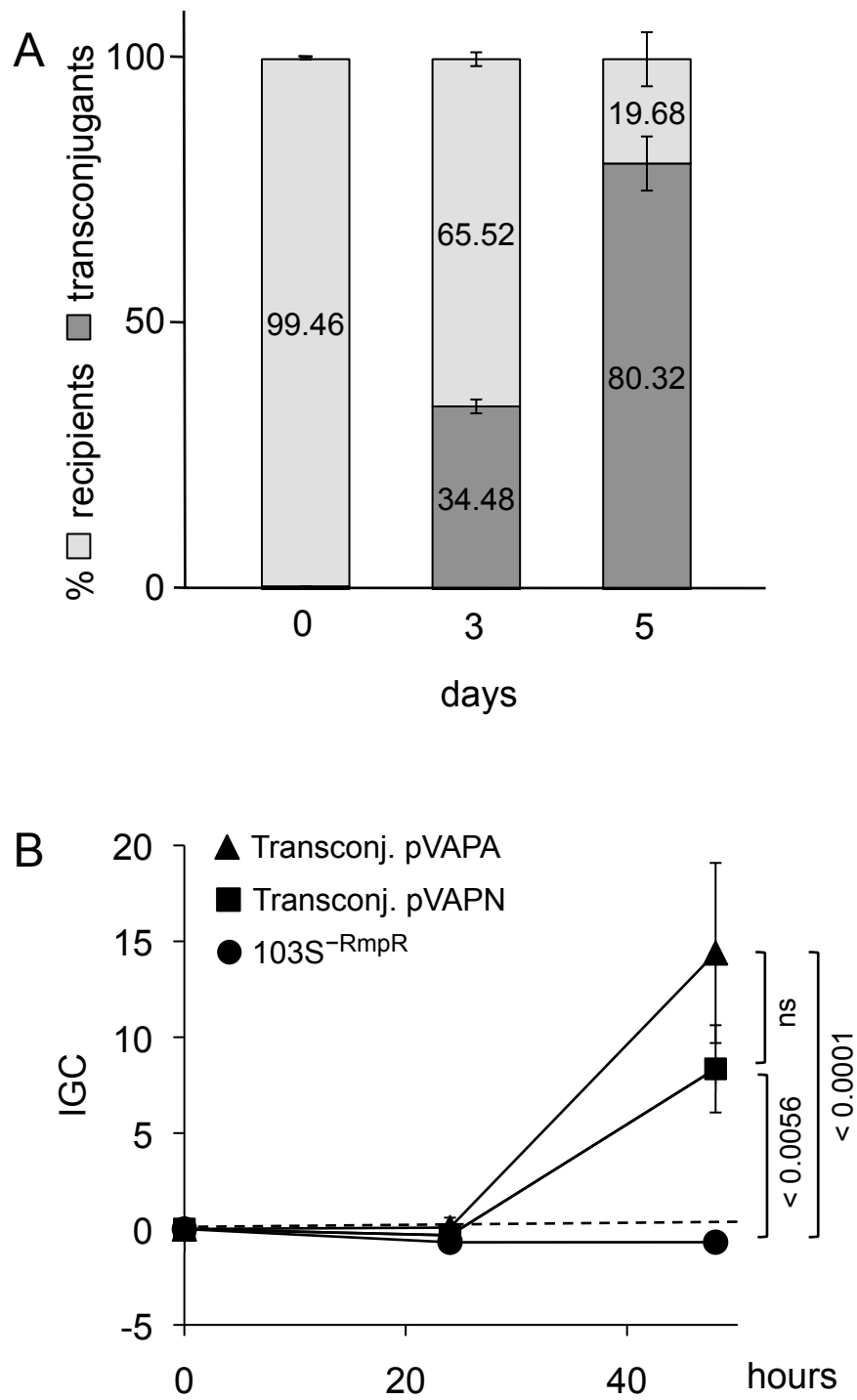


Fig. 9